UNIVERSIDADE D
COIMBRA

Gabriela dos Santos Moço

Synthesis and Screening of Derivatives of a Natural Compound with Anti-Inflammatory Activity

Dissertação no âmbito do Mestrado em Farmacologia Aplicada orientada pela Professora Doutora Alexandrina Ferreira Mendes e pelo Professor Doutor Alcino Jorge Leitão e apresentada à Faculdade de Farmácia da Universidade de Coimbra.

Outubro de 2021

UNIVERSIDADE D
COIMBRA

Gabriela dos Santos Moço

SYNTHESIS AND SCREENING OF DERIVATIVES OF A NATURAL COMPOUND WITH ANTI-INFLAMMATORY ACTIVITY

Dissertação no âmbito do Mestrado em Farmacologia Aplicada orientada pela Professora Doutora Alexandrina Ferreira Mendes e pelo Professor Doutor Alcino Jorge Leitão e apresentada à Faculdade de Farmácia da Universidade de Coimbra

Outubro de 2021

"Nothing in life is to be feared, it is only to be understood. Now is the time to understand more, so that we may fear less."

Marie Curie

Agradecimentos/ Acknowledgements

Após uma longa caminhada repleta de desafios, termino assim mais uma etapa académica que culminou com a realização da presente Dissertação. Esta jornada contou com importantes apoios, sem os quais não se teria tornado uma realidade, e aos quais estou eternamente grata.

Agradeço primeiramente aos meus orientadores, Professora Doutora Alexandrina Ferreira Mendes e Professor Doutor Alcino Jorge Leitão, por todo o apoio prestado, pela disponibilidade, pelos ensinamentos que me transmitiram e, principalmente, por me terem proporcionado a oportunidade de fazer parte de um projeto tão fascinante.

Agradeço à Doutora Cátia Moreira de Sousa, pelo auxílio incansável, pela boa disposição contagiante e pela constante presença nos momentos mais críticos deste percurso. Quem tem uma Doutora Cátia por perto, tem tudo!

Agradeço também à Sara Moura, colega do laboratório de Química Farmacêutica e, acima de tudo, amiga, por toda a ajuda que me proporcionou ao longo deste ano, sempre de boa vontade e com um enorme sorriso na cara. Obrigada por todos os bons momentos que passámos juntas no laboratório.

Às minhas colegas e amigas do laboratório de Imunologia Celular e Oncobiologia, Eliana Barbosa, Inês Rodrigues e Jéssica Macedo, pois esta jornada não teria sido a mesma sem vocês. Obrigada por terem estado sempre presentes, por terem tornado os meus dias mais alegres e por todo o apoio.

À Ana Rocha, à Inês Ribeiro e à Maria Aquino, obrigada pela vossa sincera amizade. Sei que, mesmo tendo tido poucas oportunidades para estar convosco, vocês estiveram sempre à distância de um clique.

Ao Núcleo de Estudantes de Farmácia da Associação Académica de Coimbra (NEF/AAC), por todas as incríveis oportunidades que me proporcionou enquanto Dirigente Associativa. Foi um enorme orgulho fazer parte desta Casa durante três anos, que me permitiu crescer a nível académico e pessoal. Obrigada a todos aqueles que, também fazendo parte do NEF/AAC, se cruzaram no meu caminho.

Ao meu namorado, Vítor Jesus, por ser um dos meus maiores apoios e por me fazer sorrir, mesmo nos momentos mais difíceis. Obrigada por todo o carinho que me dás e pela confiança que depositas em mim. Sinto-me sortuda por te ter a meu lado.

Aos meus pais e avós, pois sem eles, nada disto teria sido possível. Agradeço do fundo do coração pelo apoio incondicional ao longo de todo o meu percurso académico, e por me terem ajudado a tornar este sonho numa realidade.

Por último, mas não menos importante, deixo o meu mais sincero e profundo agradecimento à pessoa mais especial na minha vida. Obrigada mãe, por seres o meu pilar, o meu porto de abrigo, por me incentivares a lutar pelos meus objetivos e por estares sempre presente. És uma verdadeira inspiração!

Abbreviations

AD – Alzheimer's disease

ANOVA – Analysis of variance

ASC – Apoptosis-associated speck-like protein

BBB – Blood brain barrier

BH_4 – Tetrahydrobiopterin

BrDU – 5-bromo-2'-deoxyuridine

CaM – Calmodulin

COPD – Chronic obstructive pulmonary disease

COX-1 – Cyclooxygenase-1

COX-2 – Cyclooxygenase-2

CTs – Corticosteroids

CV – Cardiovascular

DAMPs – Damage-associated molecular patterns

DC – Dendritic cell

DEPT – Distortionless enhancement by polarization transfer

DET – Diethyl tartrate

DMAP – 4-dimethylaminopyridine

DMEM – Dulbecco's modified eagle medium

DMSO – Dimethyl sulfoxide

EdU - 5-ethynyl-2'-deoxyuridine

EtOH – Ethanol

FAD – Flavin adenine dinucleotide

FBS – Fetal bovine serum

FMN – Flavin mononucleotide

FT-IR – Fourier-transform infrared spectroscopy

GC – Glucocorticoid

GI – Gastrointestinal

GM-CSF – granulocyte-macrophage colony-stimulating factor

HEME – Protoporphyrin IX

HPA-axis – Hypothalamic-pituitary-adrenal axis

HTS – High throughput screening

IFN-γ – Interferon gamma

IKK – IκB kinase

IL-1 – Interleukin-1

IL-1R1 – IL-1 receptor type 1

iNOS – Inducible nitric oxide synthase

IR – Infrared

J – Coupling constant

L-ARG – L-arginine

LPS – lipopolysaccharide

m – multiplet

m-CPBA – meta-chloroperoxybenzoic acid

MeOH – Methanol

MHC – Major histocompatibility complex

MMPs – Matrix metalloproteinases

NADPH – Nicotinamide adenine dinucleotide phosphate

NEMO – NF-κB essential modulator

NK – Natural killer

NK-κB – Nuclear factor kappa-light-chain-enhancer of activated B cells

NLRP3 – Leucine-rich repeat pyrin-containing protein-3

NMR – Nuclear magnetic resonance

NO – Nitric oxide

NO^- – Nitrosyl anion

NO^+ – Nitrosyl cation

NSAIDs – Nonsteroidal anti-inflammatory drugs

OA – Osteoarthritis

$ONOO^-$ - Peroxynitrite

PBS – Phosphate-buffered saline

PD – Parkinson's disease

PGs – Prostaglandins

PI – Propidium iodide

PM – Primary metabolite

PS – Phosphatidylserine

RNS – Reactive nitrogen species

s – singlet

SAR – Structure-activity relationship

SEM – Standard error of mean

SM – Secondary metabolite

t – triplet

TBHP – t-Butyl hydroperoxide

THF – Tetrahydrofuran

TLC – Thin layer chromatography

TMS – Tetramethylsilane

TNF – Tumor necrosis factor

TNF-R – Tumor necrosis factor receptor

UV – Ultraviolet

V – Vehicle (0.1% DMSO)

WHO – World Health Organization

Abstract

Aging is the predominant risk factor for most chronic diseases that limit health span. As the incidence and prevalence of several chronic diseases continue to rise, interventions to increase healthy life expectancy and to delay aging are necessary.

Despite being very different, all chronic diseases have a pathophysiological mechanism in common – the occurrence of a low-grade chronic inflammation state – the occurrence of a low-grade chronic inflammation state, which contributes to their morbidity and mortality. This state is characterized by a low-grade persistent inflammatory response that frequently is not clinically evident, but can be detected by the presence of increased levels of cytokines, chemokines, prostaglandins, nitric oxide (NO), and other inflammatory mediators both in plasma and in tissues.

The current available therapeutics for inflammatory age-related diseases are only capable of reducing the symptoms related to the disease, and do not alter its course. Efforts are being made to widen the benefit-to-risk window of anti-inflammatory therapy in chronic diseases, as researchers are seeking for new classes of drugs that may be capable to stop/retard the inflammatory process related to these diseases.

Compounds of plant origin have traditionally been used against several pathologies and have recently emerged due to their diversity and large specter of benefits. Natural products have inspired many developments in medicinal chemistry, leading to advances in synthetic and semi-synthetic methodologies and to the possibility of making analogues of the original lead compounds, with improved pharmacological and/or pharmaceutical properties, based on Structure-Activity Relationship (SAR) studies.

In this project, our main goal was to design and synthetize chemical derivatives of CIAD7, a natural compound with anti-inflammatory properties, and evaluate their anti-inflammatory activity. Ten chemical derivatives of CIAD7 were synthesized, purified and their chemical structures confirmed. Four of the compounds obtained were then tested for anti-inflammatory effects and cytotoxicity.

For that, CIAD7 derivatives were evaluated for the capacity to inhibit IL-1β-induced NO production by the Griess assay, and also their effects on iNOS and pro-IL-1β protein levels by Western Blot. The anti-inflammatory properties of these compounds were studied in a mouse macrophage cell line (Raw 264.7) that was stimulated with lipopolysaccharide (LPS) of Gram-negative bacteria to induce the inflammatory response.

Viability assays showed that the chosen concentrations of the tested compounds were safe and did not present cytotoxic effects. In fact, none of the concentrations tested for all the evaluated compounds had cytotoxic effects in the presence of LPS.

The obtained results confirmed that all the test compounds are able to reduce LPS-induced iNOS protein levels and NO production in a concentration-dependent manner. Nonetheless, these compounds show significant differences in potency relative to their ability to inhibit NO production. GM23 was found to be the most potent (IC_{50}= 436.5 μM), followed by its enantiomer, GM22 (IC_{50}= 521.8 μM) and with much lower potencies, by GM16f1 (IC_{50}= 1010 μM) and GM2 (IC_{50}= 1046 μM).

This study paves the way for further *in vitro* studies aimed at fully understanding the anti-inflammatory effects of the tested compounds and the underlying mechanisms and determining whether the chemical modifications of CIAD7 introduced have any advantages over the parent compound.

Keywords: Aging; Chronic inflammation; Chemical synthesis; Natural compounds; Anti-inflammatory activity.

Resumo

O envelhecimento é o fator de risco predominante para a maioria das doenças crónicas que condicionam a esperança de vida com saúde. Uma vez que a incidência e a prevalência de várias doenças crónicas continuam a aumentar, são necessárias intervenções que permitam aumentar a expectativa de vida saudável e retardar o envelhecimento.

Apesar de bastante diferentes, todas as doenças crónicas têm um mecanismo fisiopatológico em comum – a ocorrência de inflamação crónica de baixo grau que contribui para a morbilidade e mortalidade que lhes estão associadas. A inflamação crónica de baixo grau é uma resposta persistente, de baixa intensidade e clinicamente pouco evidente, mas que pode ser detetada pelo aumento dos níveis de citocinas, quimiocinas, prostaglandinas, óxido nítrico (NO), entre outros mediadores inflamatórios, tanto no plasma como nos tecidos.

As atuais terapias disponíveis para as doenças crónicas relacionadas com o envelhecimento são apenas sintomáticas, e não alteram o curso das mesmas. Têm sido feitos esforços para alargar a janela de benefício-risco das terapias anti-inflamatórias para as doenças crónicas, visto que a comunidade científica tem investigado novas classes de medicamentos que poderão ser capazes de travar/retardar os processos inflamatórios relacionados com estas doenças.

Os compostos de origem natural têm sido tradicionalmente utilizados em diversas patologias e reemergiram recentemente devido à sua diversidade e largo espetro de benefícios. Os produtos naturais têm sido uma fonte de inspiração no desenvolvimento da química medicinal, proporcionando avanços nas metodologias sintéticas e semi-sintéticas e a possibilidade de criar análogos de compostos *lead*, com melhores características farmacológicas e/ou farmacêuticas, com base em estudos de Relação Estrutura-Atividade (REA).

Neste projeto, o nosso principal objetivo focou-se no *design* e na síntese de derivados do CIAD7, um composto natural com propriedades anti-inflamatórias, e na avaliação da atividade anti-inflamatória dos mesmos. Foram sintetizados e purificados 10 derivados do CIAD7, posteriormente confirmando as suas estruturas químicas. Quatro dos compostos obtidos foram avaliados quanto à sua citotoxicidade e efeitos anti-inflamatórios.

Para tal, os derivados do CIAD7 foram testados quanto à sua capacidade para inibir a produção de NO induzida pela IL-1β através do ensaio de Griess, e foram também avaliados os seus efeitos nos níveis de proteína de iNOS e IL-1β por Western Blot. Os efeitos anti-inflamatórios destes compostos foram estudados numa linha celular de macrófagos murinos

(Raw 264.7) que foi estimulada com lipopolissacarídeo (LPS) de bactérias Gram-negativas para induzir uma resposta inflamatória.

Os ensaios de viabilidade mostraram que as concentrações selecionadas dos compostos testados não apresentaram efeitos citotóxicos. De facto, nenhuma das concentrações testadas apresentou efeitos citotóxicos na presença de LPS para todos os compostos avaliados.

Os resultados obtidos confirmaram que todos os compostos testados têm a capacidade de reduzir os níveis de iNOS e de produção de NO, induzidos pelo LPS, de uma forma dependente da concentração. No entanto, os compostos demonstraram diferenças significativas relativamente à sua potência para inibir a produção de NO. O composto GM23 foi considerado o mais potente (IC_{50}= 436,5 μM), seguido do seu enantiómero, GM22 (IC_{50}= 521,8 μM) e com potências bastante mais baixas, os compostos GM16f1 (IC_{50}= 1010 μM) e GM2 (IC_{50}= 1046 μM).

Este estudo abre portas para futuros estudos *in vitro* com o objetivo de compreender totalmente os efeitos anti-inflamatórios dos compostos testados e os mecanismos subjacentes, podendo assim determinar se as modificações químicas introduzidas na molécula do CIAD7 têm alguma vantagem em relação ao composto original.

Palavras-chave: Envelhecimento; Inflamação crónica, Síntese química; Compostos naturais; Atividade anti-inflamatória.

List of figures

Table of contents

1. Introduction

1.1 Aging

Aging is the predominant risk factor for most chronic diseases that limit health span. As the incidence and prevalence of several chronic diseases, such as Alzheimer's disease (AD), Parkinson's disease (PD), obesity, type 2 *Diabetes Mellitus*, chronic obstructive pulmonary disease (COPD), osteoarthritis (OA), several types of cancer, among many others, continue to rise, interventions to increase healthy life expectancy and to delay aging are needed (Barbé-Tuana *et al.*, 2020; Kennedy *et al.*, 2014).

The process of aging affects all cells, tissues, organs and individuals, leading to a diminished homeostasis and increased organ frailty, causing a reduction of the response to environmental stimuli which is generally associated with an increased predisposition to illness and death (Candore *et al.*, 2010).

1.2 Inflammation

Despite being very different, all these diseases have something in common – the occurrence of a low-grade chronic inflammation state, which contributes to their morbidity and mortality. This state is characterized by a low-grade persistent inflammatory response that frequently is not clinically evident, but can be detected by the presence of increased levels of cytokines, chemokines, prostaglandins, nitric oxide (NO), and other inflammatory mediators both in plasma levels and in tissues (Mendes, Cruz and Gualillo, 2018).

The reason why specific mechanisms of inflammation are connected with chronic diseases and why older people tend to have a proinflammatory state remains unclear, and this is why researchers have been targeting this area of studies. It is important to understand the interactions that occur between the several comorbidities and the decrease of longevity and physical and cognitive decline (Bektas *et al.*, 2018).

To fully understand the pathophysiology of inflammation, it is essential to know the cells that are involved in the inflammatory mechanisms and their functions. The immune system cells play an important role in the inflammatory process. When there is tissue damage, the cells release factors called Damage-associated Molecular Patterns (DAMPs) that trigger the inflammatory cascade, along with growth factors and chemokines, which attract neutrophils. These are followed by monocytes, lymphocytes – natural killer (NK) cells, T cells and B cells, and mast cells. Monocytes can differentiate into macrophages and dendritic cells

(DC) and are recruited via chemotaxis (Chen *et al.*, 2018; Linthout, Van, Miteva and Tschöpe, 2014).

Among those cells, neutrophils act as a first-line defense are the most abundant type of leukocytes. They initiate the inflammatory response to engulf dead cells in order to promote tissue repair. However, persistent neutrophil infiltration or their delayed elimination exacerbates the tissue injury due to the release of inflammatory mediators, which is observed in chronic inflammatory responses (Germic *et al.*, 2019; Linthout, Van, Miteva and Tschöpe, 2014; Okeke and Uzonna, 2019).

Monocytes circulate in the blood, bone marrow, and spleen and do not proliferate in a steady state. They are equipped with chemokine receptors and pathogen recognition receptors that mediate their migration from blood to tissues. Monocytes have the capacity to differentiate into DCs or macrophages during the inflammatory process (Geissmann *et al.*, 2010). One of the most important roles of macrophages is the maintenance of homeostasis via phagocytosis of foreign matter, apoptotic or necrotic cells. Phagocytosis is the main mechanism for engulfment and disposal of unwanted and potentially harmful materials out of the cell (Germic *et al.*, 2019; Okeke and Uzonna, 2019). Macrophages also have the role of presenting antigens to T and B cells and secrete several cytokines (e.g., TNF-α, IL-1, IL-6, IL-8, IL-12, etc.), which direct the responses of T and B cells (Cavaillon, 1994; Okeke and Uzonna, 2019). Dendritic cells (DCs) are responsible for the first recognition of pathogens, antigen processing and regulation of T and B cells. They are equipped with high phagocytic activity when in its immature form and high cytokine producing capacity as mature cells (Fuentes *et al.*, 2017; Geissmann *et al.*, 2010).

When these coordinated mechanisms fail, and inflammation cannot be suppressed properly, there is a progression to the chronic inflammatory state (Chen *et al.*, 2018), associated with many diseases.

1.3 NF-κB

It is crucial to mention the importance of the transcription factor, Nuclear Factor kappa-light-chain-enhancer of activated B cells (NF-κB), in the pathophysiology of inflammation, as it is considered the master regulator of inflammation, playing a critical role in the control of cell death pathways and cell proliferation (Adli *et al.*, 2010).

NF-κB promotes the transcription of several genes critical for inflammatory processes including cytokines and cytokine receptors, (IL-2, IL-2 receptor, IL-6, IL-8, TNF-α, TNF-β, GM-CSF, etc.), acute phase reaction proteins, adhesion molecules, oncogenes, the major

histocompatibility complex (MHC) and proteases, among others. Indeed, the activation of NF-κB-dependent genes is a major culprit in the widespread systemic inflammatory process (Bours *et al.*, 1994; Forman *et al.*, 2016; Helenius, Kyrylenko and Salminen, 2001).

NF-κB is a pleiotropic transcription factor complex which controls the expression of numerous genes through binding to specific DNA sequences (named κB sites) inside the gene's promoters. The NF-κB family of proteins is composed of two subfamilies: The "NF-κB" proteins and the "Rel" proteins. All of these share a domain called the Rel homology domain (RHD) necessary for DNA-binding and dimerization (Bours *et al.*, 1994; Gilmore, 2006).

The NF-κB transcription factor family can be divided into two subfamilies according to their function and structure. The NF-κB subfamily is composed by p50 and p52 proteins and their precursors (p105 and p100, respectively). These two proteins don't harbor any transactivation domains and they can bind DNA as homodimers, so they function as inhibitors of the NF-κB-mediated transactivation. The Rel subfamily is formed by three proteins – RelA (or p65), RelB and c-Rel – which contain unrelated transactivation domains. RelA and c-Rel can bind DNA and transactivate as homodimers; however, the most potent NF-κB complexes are composed of heterodimers containing one protein of each group (Bours *et al.*, 1994).

The active NF-κB complex is either a homo or heterodimer composed of proteins from the NF-κB/Rel family. The affinity of specific NF-κB factors for different DNA κB sites is determined by the different combinations of NF-κB/Rel proteins in dimers (Budunova *et al.*, 1999; Gilmore, 2006).The activity of NF-κB is regulated by the interaction with another family of proteins: the IκB family. The three IκB proteins (α, β and γ) have different affinities for individual NF-κB dimers.

In most cells, NF-κB is present as a latent, inactive, IκB-bound complex in the cytoplasm. Following the classic "canonical" signaling pathway, NF-κB activation involves the activation of the IκB kinase (IKK) complex, which consists of two catalytic kinase subunits – IKKα and/or IKKβ – and a scaffold/sensing protein named NF-κB Essential Modulator (NEMO). Pro-inflammatory signals stimulate receptors belonging to the tumor necrosis factor receptor (TNF-R) or interleukin-1 (IL-1)/Toll-like receptor (TLR) superfamilies, which activate the IKK complex. Its activation leads to IκB phosphorylation and subsequent ubiquitin-dependent IκB degradation by the 26S proteosome complex, which enables the NF-κB dimers to enter the nucleus and activate genes with mainly pro-inflammatory and anti-apoptotic functions (Adli *et al.*, 2010; Gilmore, 2006; Pasparakis, 2009).

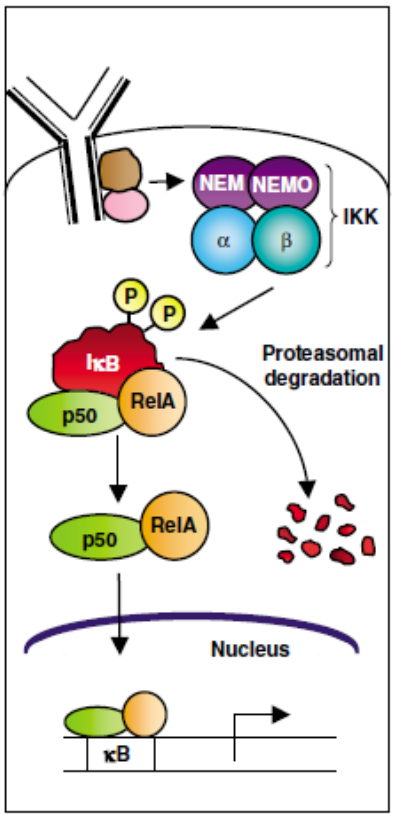

Figure 1. Canonical NF-kB signaling pathway. NF-kB dimers such as p50/RelA are maintained in the cytoplasm by interaction with an independent IkB molecule (often IkBα). In many cases, the binding of a ligand to a cell surface receptor (e.g., TNF-R or TLR) recruits adaptors to the cytoplasmic domain of the receptor. In turn, these adaptors often recruit an IKK complex (containing the α and β catalytic subunits and two molecules of the regulatory scaffold NEMO) directly onto the cytoplasmic adaptors. This clustering of molecules at the receptor activates the IKK complex. IKK then phosphorylates IkB at two serine residues, which leads to its ubiquitination and degradation by the proteasome. NF-kB then enters the nucleus to turn on target genes.
Adapted from Gilmore, 2006.

1.4 iNOS

One of the genes activated by the NF-κBs pathway is Nos2, which codes for the inducible Nitric Oxide Synthase (iNOS) enzyme. iNOS is responsible for the synthesis of NO and is implicated in the pathophysiology of several inflammatory diseases. NF-κB has been shown to be a central target for stimuli that activate or inhibit iNOS expression (Oh *et al.*, 2008). NO has a very short half-life of only a few seconds, but it is a highly reactive molecule. Alongside with its derivatives – nitrosyl cation (NO^+), nitrosyl anion (NO^-) and peroxynitrite ($ONOO^-$) – they can cause the formation of new reactive nitrogen species (RNS) and react with cell proteins and impair cell function (Kielbik, Szulc-Kielbik e Klink, 2019; Król e Kepinska, 2021).

The iNOS monomer has three domains – the oxygenase domain, the reductase domain, and the calmodulin-binding domain. The first one is responsible for binding tetrahydrobiopterin (BH_4), L-arginine (L-ARG) and protoporphyrin IX (HEME). The second

one consists of binding sites for flavin mononucleotide (FMN), flavin adenine dinucleotide (FAD) and nicotinamide adenine dinucleotide phosphate (NADPH), that play the role of functional groups, transporting electrons from NADPH to the oxygenase domain of the opposite subunit. The calmodulin (CaM) domain is noncovalently bound to the iNOS monomer (Kielbik, Szulc-Kielbik and Klink, 2019; Król and Kepinska, 2021).

Unlike the constitutive NOS isoforms, iNOS doesn't need an increase in the Ca^{2+} levels to initiate its activity and can produce large and toxic amounts of NO during the course of inflammatory response, until the enzyme is degraded. It is activated by numerous stimuli, including inflammatory cytokines, like IFN- γ, TFN-α or IL-1β, and microbial products, such as bacterial lipopolysaccharide (LPS) (Guzik e Korbut, 2003; Kleinert, Art and Pautz, 2010).

Pro-inflammatory cytokines, such as TNF-α, IL-1β, IFN-γ, and LPS, first bind to receptors on the cell surface and activate kinases leading to phosphorylation of several intracellular proteins and subsequent activation of specific transcription factors, including NF-κB transcription factors. The active factors then translocate to the nucleus and bind to the promoter region of Nos2, inducing iNOS expression (Cinelli *et al.*, 2020). IL-1β, TNF-α and oxidative stress induce NF-κB activity and its translocation to the nucleus, subsequently inducing its binding to the promoter sequence (Kielbik, Szulc-Kielbik and Klink, 2019).

As said before, TNF-α, IL-1β, IFN-γ, and LPS are the main inducers of iNOS expression. It is important to mention that a combination of these inducers is frequently required to generate synergistic effects most of the times to stimulate iNOS expression, especially in nonimmune cells (Cinelli *et al.*, 2021; Kleinert, Art and Pautz, 2010).

1.5 IL-1β

IL-1β is another very important inflammatory cytokine. IL-1 is a central mediator of immunity and inflammation; there are two different genes, IL1A and IL1B, encoding IL-1α and IL-1β respectively. Each IL-1 binds to the same cell surface receptor, named IL-1 receptor type 1 (IL-1RI), which is present on almost all cells. Once linked to its receptor, the cytokine triggers a cascade of inflammatory mediators, chemokines and other cytokines. In this project, I will give focus to IL-1β, which is produced by hematopoietic cells such as blood monocytes, tissue macrophages, skin dendritic cells, and brain microglia in response to toll-like receptors (TLR), activated complement components, other cytokines (e.g., TNF-α), and IL-1 itself (Dinarello, Simon and Meer, van der, 2012; Garlanda, Dinarello and Mantovani, 2013).

IL-1β is not active by itself but can be activated when cleaved by caspase-1, an intracellular cysteine protease, converting the inactive precursor of IL-1β (pro-IL-1β) to the

active form and releasing it into the extracellular space. Caspase-1 also requires activation, which occurs following the assembly of a complex of intracellular proteins called the inflammasome. The key component of this complex is the protein-nucleotide-binding domain and leucine-rich repeat pyrin-containing protein-3 (NLRP3) (Dinarello, Simon and Meer, van der, 2012; Garlanda, Dinarello and Mantovani, 2013).

Inflammasomes are cytosolic wheel-like complexes composed by the junction of NACHT, LRR and PYD domains-containing proteins (NLRP), the linker molecule apoptosis-associated speck-like protein (ASC), and caspase-1. NLRP1 and NLRP3 are the ones with the capacity to translate a wide variety of danger signals into the caspase-1–dependent secretion of IL-1β. Furthermore, its release promotes the production and release of several inflammatory mediators and catabolic factors, such as iNOS, PGE_2, TNF-α and matrix metalloproteinases (MMPs) (Anders, 2016; Fei *et al.*, 2019).

1.6 Limitations of the current therapies

Nowadays, the available therapeutics for inflammatory age-related diseases are only capable of controlling the symptoms related to the disease, and do not alter its course. Efforts are being made to widen the benefit-to-risk window of anti-inflammatory therapy in chronic diseases, as researchers are seeking for new classes of drugs that may be capable to stop/retard the inflammatory stimulus related to these diseases (Tabas and Glass, 2013).

Nonsteroidal anti-inflammatory drugs (NSAIDs) are probably the most popular option, as they have the capability to decrease pain and reduce inflammation. Their general mode of action involves the inhibition of cyclooxygenase/prostaglandin-endoperoxide synthase (COX-1 and COX-2), regulatory enzymes, involved in the biosynthesis of prostaglandins (PGs) which are strongly implicated in the pathophysiology of inflammation (Bindu, Mazumder and Bandyopadhyay, 2020).

Unfortunately, NSAIDs can cause several complications when used for long periods of time. They are known to pose a risk to the gastrointestinal (GI) system, particularly non-selective NSAIDs, but now it is known that COX-2 inhibitors also increase the risk of upper GI problems. The development of gastric mucosal injury creates the major limitation to this drug class. Long-term use of NSAIDs severely increases the risk of occurring CV events, especially with COX-2 inhibitors. For individuals who present several risk factors of CV disease, short-term consumption of NSAIDs highly increases the risk of a CV occurrence. Other negative effects may also include nephrotoxicity and consequent chronic renal failure

and hepatotoxicity (Bindu, Mazumder and Bandyopadhyay, 2020; Cooper *et al.*, 2019; Ohadoma, Akah and Michael, 2020).

Corticosteroids (CTs) are another therapeutical option for inflammatory diseases. They are synthetic analogues of the natural steroid hormones produced by the adrenal cortex, so just like the natural hormones, these synthetic versions have glucocorticoid (GC) and/or mineralocorticoid properties (Liu *et al.*, 2013).

Like NSAIDs, GCs have a vast list of side effects when used for a long time. Patients who are subjected to long-term GC treatment may experience various systemic effects and these seem to be dose-dependent. Long-term GC therapy may cause disturbed wound healing, permanent striae, skin atrophy, myopathy, cataracts, glaucoma, psychiatric disturbances (or aggravation of pre-existing disturbances), induction or aggravation of pre-existing diabetes, adrenal insufficiency, hypogonadism, Cushing's syndrome, peptic ulcers, upper gastrointestinal bleeding, pancreatitis, hypertension, dyslipidemia, reduced fibrinolytic potential, weight gain, HPA-axis suppression, higher risk of CV diseases, including hypertension, and increased risk of infection, among others (Adcock and Mumby, 2016; Barnes, 2006; Liu *et al.*, 2013; Schäcke, Döcke and Asadullah, 2002).

1.7 Products of natural sources

Since the available therapeutics for the management of chronic inflammation are not very effective due to their mass list of side effects, the scientific community has been putting effort on finding new alternatives. Compounds of plant origin have traditionally been used against several pathologies and have recently emerged due to their diversity and large specter of benefits. World Health Organization (WHO) has estimated that in 1985, approximately 65% of the world population depended on traditional plant-based medicines. Medicinal plants represent an important source of compounds and are cultivated worldwide to obtain useful substances in medicine and pharmacy (Cragg and Newman, 2013; Kang, 2021; Prasad, Sung and Aggarwal, 2012; Salmerón-Manzano, Garrido-Cardenas and Manzano-Agugliaro, 2020).

1.8 Secondary metabolites

Plants contain reservoirs of potential secondary metabolites (SMs) that are the major sources of drugs, which intensifies the interest of pharmaceutical industries in the search for substances obtained from plant sources. The principal objectives of the use of plants as therapeutic agents are the following: to isolate bioactive substances for direct use as drugs; to produce bioactive compounds of new or already known structures for semi-synthesis to

produce patentable entities of higher activity and/or lower toxicity; and to use the whole plant or parts of it as herbal remedies (Azab, Nassar and Azab, 2016).

Primary metabolites (PMs) – nucleic acids, proteins, carbohydrates, fats and lipids – are found in all plants and have a crucial role in plant development, as they are involved in metabolic, nutritional and reproduction functions. SMs are not necessary for the plant to live, but play an important role in the interaction of the organism with its surroundings, ensuring the continued existence of the organism in its ecosystems. Formation of SMs is generally organ, tissue and cell specific and contributes for the species' survival. SMs can be separated into four groups – Terpenoids, Polyketides, Phenypropanoids and Alkaloids – based on their biosynthesis origin. Alkaloids are nitrogenous organic molecules biosynthesized mainly from amino-acids, and many of the most important therapeutic agents are alkaloids (Pagare *et al.*, 2015).

SMs have several functions. They constitute a mean for plants to defend themselves against biotic (bacteria, fungi, insects, animals, etc.) and abiotic (higher temperature and moisture, presence of heavy metals, UV radiation, etc.) stresses. Some SMs also serve as signal compounds to attract pollinating and seed-dispersing animals (Kinghorn, 2002; Pagare *et al.*, 2015; Wink, 2015).

Biosynthesis of SMs starts from basic pathways, such as the glycolysis or shikimic acid pathways, and subsequently diversifies, depending on cell type, developmental stage and environmental conditions. SMs are widely distributed in different plants cells, tissues and organs. However, different cells, tissues and organs of medicinal plants may possess different medicinal properties at different developmental stages. Furthermore, plant growth and development are usually conditioned by different environmental changes. The adaptation of plant morphology, anatomy, and physiological functions to these changes may influence the accumulation of SMs. SM pathways and their regulation are susceptible to environmental variations because the expression of genes involved in SM pathways are altered by different stresses (Li *et al.*, 2020).

Synthesis and accumulation of SMs are controlled and influenced by the changing of biotic and abiotic environment. During their development, plants interact with the surrounding environment, coming in contact with different abiotic components like water, light, temperature, soil and chemicals. Negative abiotic factors, such as drought or flooding, extremes of light and temperature and the presence of poor soil or toxic chemicals generate stress and trigger variation in the biosynthesis of SMs (Li *et al.*, 2020).

1.9 Drug discovery

Research into natural products provides new lead compounds for the pharmaceutical industry. It is undeniable that natural products have been key sources of innovative therapeutic agents (Mathur and Hoskins, 2017). Natural products have inspired many developments in organic chemistry, leading to advances in synthetic and semi-synthetic methodologies and to the possibility of making analogues of the original lead compounds, with improved pharmacological and/or pharmaceutical properties (Harvey, 2008). These compounds can also serve as an inspiration, by providing insight into types of structural features that may prove valuable for drug candidates that, in this case, have been designed based on a natural product, but are not themselves synthesized from that natural compound (Wilson and Danishefsky, 2006).

Products of natural sources have molecular structures that range from very simple arrangements to extremely complex. However, with improvements in structure-activity studies, it has been possible to synthetize these compounds in the laboratory. Total synthetic approaches to natural compounds are getting more viable as a sourcing option and given sufficient resources, it will be possible to reduce the number of synthetic steps to the target molecule and improve the yield of each step (Beutler, 2009).

During the early stages of the drug discovery process, scientists have to isolate and purify the lead compounds from their natural sources using various techniques, depending on the structural diversity, stability and quantity of the compound required. High throughput screening (HTS) has been used to screen the lead compounds against specific targets, and promising compounds for the specific targets are selected in cell-free assays and/or phenotypic or targeted cell-based assays (Henrich and Beutler, 2013). At this phase, many lead compounds are not selective enough for their target molecule. To improve their selectivity, scientists can modify the lead compound structures as per the expected structure-activity relationships. If the modifications increase the selectivity, the promising compounds can move to *in vitro* and *in vivo* testing. Further pharmacokinetic tests are also required to establish the mechanism by which the drug is absorbed, distributed, metabolized and excreted and, if these are favorable, the lead compounds may become potential drug candidates (Mathur and Hoskins, 2017).

The plant extract must be fractionated to isolate and identify the active compound(s). After that, the compounds' chemical structures can be elucidated using many techniques, but the principal one is Nuclear Magnetic Resonance (NMR). The ability of NMR to provide useful information from smaller amounts of compound has increased intensely in recent years in terms of sensitivity (Beutler, 2009). NMR experiments can be carried out under high pressure, at a wide range of temperatures and in various solvents, such as organic solvents (Li and Kang, 2020).

Despite the all the valuable assets that natural products bring into the drug discovery process and their unique structural diversity, there are still several problems associated with them, such as low solubility, insufficient efficacy, undesirable toxicity, chemical instability, among others (Xiao, Morris-Natschke and Lee, 2016). Naturally active compounds are usually good leads but most of them can hardly satisfy the demands for druggability, so they are frequently optimized through structural modifications in order to achieve the final candidate (Chen *et al.*, 2015).

The optimization of natural lead structures must involve efforts on the following purposes: enhancing drug efficacy, increasing potency and selectivity, optimizing absorption, distribution, metabolism, excretion profiles (ADME), reducing toxicity and eliminating and/or reducing side effects. Natural lead optimization generally involves the initial establishment of structure-activity relationships (SAR) between the chemical structures of the compounds and their biological activities (Chen *et al.*, 2015; Xiao, Morris-Natschke and Lee, 2016).

The goal of developing SARs is to understand and reveal how properties relevant to the biological activity of the compounds are encoded within and determined by their chemical structures. Therefore, molecular alterations based on SAR can be established to ensure more rational optimization of the natural leads (McKinney *et al.*, 2000; Xiao, Morris-Natschke and Lee, 2016).

1.10 Compound modification strategies

There are several possible modification strategies when it comes to the development of new drugs. In this project, I will briefly mention some of the most common strategies used and highlight their advantages.

1.10.1 Manipulation of the molecular size and complexity

When natural products present very large and complex structures with higher molecular weights (Yao *et al.*, 2017), simplifying operations such as molecular dissection are generally carried out in order to eliminate structurally-unnecessary factors. In the case of compounds with fused rings, the scaffolds can be segmented into four quadrants to separately modify the structures/groups, always maintaining SAR. The usage of the principles of medicinal chemistry, such as bio-isosterism, chain-ring exchange, privileged structure and scaffold-hopping, allows the achievement of new analogs with better properties (Guo, 2017).

Small-size compounds have structural space to add atoms, groups or moieties. For example, introducing a hydrogen donor or acceptor group may increase the affinity to a certain

receptor, or adding solubilizing groups may raise the solubility or modulate the partition property to benefit or avoid crossing the blood brain barrier (BBB)(Guo, 2017).

1.10.2 Improvement of chemical stability

Chemical instability reduces the compound concentration and produces decomposition products that may be active. Oxygen, water, light, trace metals, and materials leached from plastic or glass containers can react with the compound. Structural modifications that can improve chemical stability depend mainly on the unstable functional groups that must be replaced, eliminated or modified (Chen *et al.*, 2015).

1.10.3 Improvement of plasma stability

Compounds with certain functional groups can decompose in the bloodstream. Unstable compounds often have high clearance and a short half-life, leading to a poor pharmacological performance. The plasma stability can be increased by substituting an amide for an ester or eliminating a hydrolysable group (Chen *et al.*, 2015).

1.10.4 Increase of low solubility

Low water solubility limits absorption depending on the route of administration, consequently affecting oral bioavailability. The absorption of drugs by passive diffusion depends on the concentration gradient between the intestinal lumen and the blood, which is a process influenced by solubility. Thus, it is important to find strategies to increase aqueous solubility without lowering hydrophobicity (Morimoto *et al.*, 2021). Structural modifications that improve solubility normally include adding ionizable or polar groups, like adding a basic amine or a carboxylic acid (Chen *et al.*, 2015).

1.10.5 Improvement of metabolic stability

Many natural compounds that are highly active *in vitro* may have limited activity *in vivo* due to their susceptibility to metabolism. Drug metabolism is divided into two phases – I and II. Phase I metabolism includes mainly reduction and oxidation reactions, while phase II metabolism contains reactions of glucuronidation and sulfation. These processes increase clearance, reduce exposure, and are a major cause of low bioavailability. Structural modifications that reduce compound binding or reactivity at the labile site will increase metabolic stability. For example, blocking the metabolic site by adding other blocking groups

or removing labile functional groups and replacing unstable groups may be good strategies to achieve stability (Chen *et al.*, 2015; Yao *et al.*, 2017).

1.11 CIAD7

CIAD7 is a small natural compound that has previously shown to have anti-inflammatory properties. However, its high volatility and low molecular weight have a slight negative impact on its druggability. In order to improve CIAD7's chemical profile and based on previous SAR studies, we decided to proceed with two different molecular modification approaches:

a) Removing the double bond and adding a hydroxyl group or;
b) Adding either a hydroxyl or an ether group, via an epoxide.

Due to previous studies, we decided not to modify the ring structure, represented by R, because it is known that alterations in that part of the molecule may decrease or eliminate the compound's pharmacological activity. With these modifications, we aimed to decrease CIAD7 volatility and increase its molecular weight as well. Further molecular alterations were made until we reached our final compounds, and some of them were evaluated biologically to better understand their anti-inflammatory characteristics, comparing to CIAD7. Both enantiomers of CIAD7 are represented below (Figures 2 and 3).

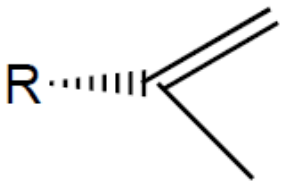

Figure 3. R-(-)-CIAD7

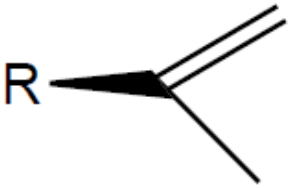

Figure 2. S-(+)-CIAD7

2. Main objectives

Due to the limitations of the available therapies for inflammatory diseases, which focus mainly on treating symptoms and not the cause of inflammation itself, it is crucial to find new medicines that may be capable of interfering with the mechanisms associated with inflammation more effectively. Medicinal plants offer a great variety of compounds that have shown anti-inflammatory properties and several studies have been conducted to further understand their effects.

Chemical alterations allow the obtention of compounds with improved pharmacokinetic and pharmacodynamic properties, which may improve their pharmacotherapeutic characteristics. CIAD7 is a natural compound that has previously shown anti-inflammatory properties. In this project, our main goal was to design and synthetize CIAD7 chemical derivatives through selected chemical modifications and evaluate their anti-inflammatory activity. Ten chemical derivatives of CIAD7 were synthesized, purified and their chemical structures confirmed. The compounds obtained were then tested for anti-inflammatory effects and cytotoxicity. For that, CIAD7 derivatives were evaluated for the capacity to inhibit IL-1β-induced NO production by the Griess assay, and also their effects on iNOS and pro-IL-1β protein levels by Western Blot. The anti-inflammatory properties of these compounds were studied in a mouse macrophage cell line (Raw 264.7) that was stimulated with lipopolysaccharide (LPS) of Gram-negative bacteria to induce the inflammatory response.

3. Experimental procedures

3.1 Semi-synthesis of ClAD7 derivatives

3.1.1 Equipment

3.1.1.1 Chromatography

For the monitoring of the reactions by thin layer chromatography (TLC), we used silica plates 60 F_{254} with aluminum support. For column chromatography we used silica gel 60 (0.063-0.200 mm) by Merck, Germany.

3.1.1.2 Nuclear Magnetic Resonance (NMR)

NMR spectrums were obtained through the Bruker Avance III spectrometer at 400 MHz (H^1) or 100 MHz (C^{13}), and tetramethylsilane (TMS) was used as reference. Chemical shifts (δ) are reported in parts per million (ppm) and coupling constants (J) are reported in hertz (Hz).

3.1.1.3 Infrared (IR) spectroscopy

Infrared (IR) spectrums were recorded on a Fourier Transform spectrometer, Perkin Elmer Spectrum 400, using ATR.

3.1.2 Reagents and solvents

Most of the solvents and reagents are commercially available and used without further purification. Tetrahydrofuran (THF) was dried by refluxing over calcium hydride (CaH_2) for 7 h, distilled from CaH_2 and stored in molecular sieves. Methanol (MeOH) and ethanol (EtOH) were distilled, and stored in activated molecular sieves for at least 24 h before being used.

3.1.3 Methods

3.1.3.1 Hydration of (+)- and (-)-ClAD7 (GM1 and GM2)

This experimental procedure was already well established at our laboratory. ClAD7 (3.3 mmol) was added to 3.3 mL of 50% aqueous sulfuric acid (H_2SO_4) at 0 °C (ice bath) and stirred for 24 h. After the 24 h period, 6 mL of petroleum ether 60-80 and a few drops of ethyl ether were added and the mixture was kept under agitation at 0 °C for more 10 min. Then, the organic phase was removed and the aqueous phase was extracted for 24 h with

ethyl ether (3 x 6 mL). Organic phases were washed with brine (saturated aqueous sodium chloride, NaCl) and 10% aqueous sodium bicarbonate ($NaHCO_3$), then dried with anhydrous sodium sulfate (Na_2SO_4) and evaporated under reduced pressure. The aqueous phase was extracted again with ethyl acetate for 24 h (3 x 10 mL) and the organic phase was managed as previously described. Both fractions were purified by flash chromatography (eluent petroleum ether:ethyl acetate 1:0 to 1:1). The obtained product was a viscous yellow liquid, in 0.72 mmol, 22% yield, for GM1 and 0.69 mmol, 21% yield, for GM2.

Analytical data of GM1:

FT-IR (ATR): cm^{-1} = 3432 (O-H)

^{1}H NMR (400 MHz, $CDCl_3$): δ = 1.23 (3H, s, -C<u>H</u>$_3$); 1.24 (3H, s, -C<u>H</u>$_3$)

^{13}C NMR (100 MHz, $CDCl_3$): δ = 27.02 (-<u>C</u>H_3); 27.31 (-<u>C</u>H_3); 71.64 (-<u>C</u>OH)

3.1.3.2 Epoxidation of the double bond of CIAD7 – GM3 and GM4

This procedure was adapted from (Eckrich *et al.*, 1996). CIAD7 (3.3 mmol) was dissolved in 8 mL of ice-cold dichloromethane (CH_2Cl_2) and a solution of 75% meta-chloroperoxybenzoic acid (m-CPBA) (0.85 g, 3.69 mmol) diluted in 4 mL of dichloromethane, were added dropwise for 10 min. The mixture was stirred at 0 °C (ice bath) for 16 h (controlled by TLC). Once the reaction is over, the mixture was stirred with 1 mL of 10% aqueous Na_2SO_3 for 1 – 2 min, filtered and the solid residue was washed with several portions of dichloromethane. The organic phase was washed with 10% aqueous Na_2CO_3 (3 x 15 mL) and brine (15 mL), dried with anhydrous sodium sulfate, and the solvent evaporated under reduced pressure. The residue was further purified by flash chromatography (eluent petroleum ether:ethyl acetate 1:0 to 1:1), and the product was obtained as a viscous yellow liquid, in 2.17 mmol, 66% yield for GM3 and 1.95 mmol, 59% for GM4.

Analytical data of GM3:

FT-IR (ATR): cm^{-1} = 802; 829 (C-O)

^{1}H NMR (400 MHz, $CDCl_3$): δ = 1.22 (3H, s, -C<u>H</u>$_3$); 2.42 – 2.50 (2H, m, -C<u>H</u>$_2$O)

^{13}C NMR (100 MHz, $CDCl_3$): δ = 18.32 (-<u>C</u>H_3); 52.37 (-<u>C</u>H_2O); 57.78 (-<u>C</u>)

3.1.3.3 Selective opening of the epoxide with MeOH – GM10f1, GM10f2, GM16f1 and GM16f2

This procedure was adapted from (Leitão *et al.*, 2008). To a solution of GM3 (1.0 mmol) in 5 mL of MeOH it is added 13 mg of hydrazine sulfate salt ($NH_2NH_2.H_2SO_4$). After the appropriate time under magnetic stirring at 50 °C (until the reaction is completed as verified by TLC control), the reaction mixture is filtered (the catalyst is recovered) and the filtrate is concentrated under reduced pressure. The resulting residue is purified by flash chromatography (eluent petroleum ether:ethyl acetate 1:0 to 1:1), and the products were obtained as viscous yellow liquids, in 0.19 mmol, 19% yield for GM10f1 and 0.25 mmol, 25% for GM10f2.

GM4 was submitted to the same procedure as GM3. The obtained products were also viscous yellow liquids, in 0.21 mmol, 21% yield for GM16f1 and 0.28 mmol, 28% for GM16f2.

Analytical data of GM10f2:

FT-IR (ATR): cm^{-1} = 3454 (O-H); 1061 (C-O)

^{1}H NMR (400 MHz, $CDCl_3$): δ = 1.10 [1,11] (3H, s, -C$\underline{H}_3$); 3.22 [3.23] (3H, s, -OC$\underline{H}_3$); 3.50 – 3.58 (2H, m, -C$\underline{H}_2$OH)

^{13}C NMR (100 MHz, $CDCl_3$): δ = 16.55 [16.72] (-$\underline{C}H_3$); 49.49 [49.57] (-O$\underline{C}H_3$); 64.13 [64.37] (-$\underline{C}H_2$OH); 77.70 [77.74] (-$\underline{C}$)

Analytical data of GM16f1:

FT-IR (ATR): cm^{-1} = 3460 (O-H); 1107 (C-O)

^{1}H NMR (400 MHz, $CDCl_3$): δ = 1.12 [1.13] (3H, s, -C$\underline{H}_3$); 3.36 [3,37] (3H, s, -OC$\underline{H}_3$); 3.19 – 3.24 (2H, m, -C$\underline{H}_2$OH)

^{13}C NMR (100 MHz, $CDCl_3$): δ = 20.83 [21.44] (-$\underline{C}H_3$); 59.39 [59.43] (-O$\underline{C}H_3$); 72.72 [72.88] (-$\underline{C}$); 78.13 [78.13] (-$\underline{C}H_2$OH)

The values in square brackets represent each compound's diastereoisomer.

3.1.3.4 Selective opening of the epoxide with EtOH – GM13f1, GM13f2, GM17f1 and GM17f2

This procedure follows the same steps as the previous one, except for the use of 5 mL of EtOH instead of MeOH.

GM13f1 and GM13f2 were obtained from GM3, both resulting in viscous yellow liquids, in 0.08 mmol, 8% yield for GM13f1 and 0.11 mmol, 11% for GM13f2. GM17f1 and GM17f2 were obtained from GM4, also resulting in viscous yellow liquids, in 0.10 mmol, 10% yield for GM17f1 and 0.15 mmol, 15% for GM17f2.

Analytical data of GM17f2:

FT-IR (ATR): cm^{-1} = 3459 (O-H); 1061 (C-O)

^{1}H NMR (400 MHz, $CDCl_3$): δ = 1.11 [1.12] (3H, s, -C$\underline{H}_3$); 1.16 [1.17] (3H, t (J = 6.0 Hz), -OCH$_2$C$\underline{H}_3$); 3.38 – 3.44 (2H, m, -OC$\underline{H}_2$CH$_3$); 3.53 [3.53] (2H, s, -C$\underline{H}_2$OH)

^{13}C NMR (100 MHz, $CDCl_3$): δ = 15.75 [16.04] (-$\underline{C}$H$_3$CH$_2$O); 17.10 [17.49] (-$\underline{C}$H3); 56.84 [56.92] (-O$\underline{C}$H$_2$CH$_3$); 64.62 [64.99] (-$\underline{C}$H$_2$OH); 77.60 [77.60] (-$\underline{C}$)

The values in square brackets represent the compound's diastereoisomer.

3.1.3.5 Esterification of tertiary alcohols – GM22 and GM23

This procedure was adapted from (Figueiredo *et al.*, 2017). GM1 (0.59 mmol) was dissolved in 4 mL of dry tetrahydrofuran (THF). 0.4 mL of acetic anhydride ($C_4H_6O_3$) and 75 mg of 4-dimethylaminopyridine (DMAP) and stirred overnight at room temperature. The mixture was successively washed with 1M solution of acid chloride (HCl) and brine, dried with anhydrous sodium sulfate, evaporated under reduced pressure and purified by flash chromatography (eluent petroleum ether:ethyl acetate 1:0 to 1:1). GM23 consisted in a viscous yellow liquid, in 0.42 mmol, 71% yield.

GM22 was obtained through the same method from GM2. The product also consisted in a viscous yellow liquid, in 0.20 mmol, 34% yield.

Analytical data of GM22:

FT-IR (ATR): cm^{-1} = 1727 (C=O)

^{1}H NMR (400 MHz, $CDCl_3$): δ = 1.46 (6H, s, -C$\underline{H}_3$); 1.97 (3H, s, -OCOC$\underline{H}_3$)

^{13}C NMR (100 MHz, $CDCl_3$): δ = 23.30 (-$\underline{C}$H$_3$); 23.46 (-$\underline{C}$H$_3$); 44.33 (-OCO$\underline{C}$H$_3$); 82.88 (-$\underline{C}$); 199.69 (-O$\underline{C}$OCH$_3$)

3.2 Pharmacological characterization of CIAD7 derivatives

3.2.1 Cell culture and treatments

Raw 264.7 cells – a mouse macrophage cell line – were cultured in DMEM (Gibco, USA) supplemented with 10% non-inactivated fetal bovine serum (FBS; Gibco, USA), 100 U/mL penicillin (Sigma-Aldrich Co., St Louis, MO, USA) and 100 μg/mL streptomycin (Sigma-Aldrich Co.). Raw 264.7 cells were plated at a density of 3×10^5 cells/mL and left to stabilize for up to 24 h.

For cell treatments, the test compounds were dissolved in dimethyl sulfoxide (DMSO; Honeywell, Germany). LPS from *Escherichia coli* 026:B6 (Sigma-Aldrich Co.) was dissolved in phosphate-buffered saline (PBS). DMSO was used as a vehicle and added to the positive control (untreated cells + DMSO) as well as the LPS-treated cells to match the same concentration as in the cells treated with the test compounds. The final concentration of DMSO was 0.1% (v/v).

The concentrations of the test compounds were selected based on non-cytotoxic concentrations of CIAD7 previously identified by other researchers from our group. Absence of cytotoxic effects of the test compounds in those concentrations was confirmed. Test compounds or DMSO were added to Raw 264.7 cells 1 h before the pro-inflammatory stimulus, 1 μg/mL LPS, and maintained for the rest of the experimental period (18 h) at 37 °C.

3.2.2 Selection of non-cytotoxic concentrations of the test compounds by the resazurin assay

Resazurin is a redox dye used as an indicator of active metabolism with several applications, including cell viability, proliferation and toxicity studies. This assay is based on the intracellular reduction of resazurin – a non-fluorescent compound – to resorufin, a fluorescent and pink colored compound by mitochondrial or microsomal enzymes that use NADH or NADPH as electron sources. Only metabolically active cells can reduce resazurin, which means that fluorescence or absorbance intensity is directly proportional to the number of viable cells (Präbst *et al.*, 2017). By comparing the result obtained in the test condition with that observed in the control, it is possible to determine whether the test condition affects cell viability and/or proliferation. According to the standard for cytotoxicity assessment, ISO 10993-5, cell toxicity is defined as a decrease in metabolically active cells larger than 30% relative to the control condition.

The resazurin solution was added to each well to a final concentration of 50 μM, 90 min before the end of the 18 h treatment. Then, absorbances at 570 nm and 620 nm (reference wavelength) were read in a Biotek Synergy HT plate reader (Biotek, Winooski, VT, USA).

3.2.3 Preparation of cell extracts

Cell cultures were washed with ice-cold PBS and lysed with ice-cold RIPA buffer [150 mM sodium chloride (ThermoFisher Scientific), 50mMTris (ThermoFisher Scientific, pH 7.5), 5mMethylene glycol-bis(2-aminoethylether)- N,N,N',N'-tetraacetic acid (EGTA; Sigma-Aldrich Co.), 0.5% sodium deoxycholate (Sigma- Aldrich Co.), 0.1% sodium dodecyl sulfate (SDS; Sigma-Aldrich Co.), 1% Triton X-100 (Merck Millipore Ltd., Darmstadt, Germany)], supplemented with protease (Complete, Mini, Roche Diagnostics, Mannheim, Germany) and phosphatase (PhosSTOP, Roche Diagnostics, Mannheim, Germany) inhibitors, for 30 min. The lysates were then centrifuged at 14,000 rpm for 10 min at 4 °C and the supernatants were stored at -20 °C until use. Protein concentration in the extracts was determined with the bicinchoninic acid kit (Sigma-Aldrich Co.).

3.2.4 Nitric oxide production

NO production was measured based on the amount of nitrite accumulated in the culture supernatants using the Griess assay. It consists in a two-step diazotization reaction in which the NO derived nitrosating agent, dinitrogen trioxide (N_2O_3) generated from the acid-catalyzed formation of nitrous acid from nitrite (or autoxidation of NO) reacts with sulfanilamide to produce a diazonium ion which is then coupled to *N*-(1-napthyl)ethylenediamine to form a chromophoric azo product that absorbs strongly at 540 nm (Bryan and Grisham, 2007). Equal volumes of culture supernatants and reagents [equal volumes of 1% (w/v) sulphanilamide in 5% (v/v) phosphoric acid and 0.1% (w/v) N-(1-napthtyl) ethylenediamine dihydrochloride were mixed and incubated for 10 min at room temperature and placed in the dark. The concentration of accumulated nitrite in the culture supernatants was calculated by interpolation of the absorbance of each sample, read in Biotek Synergy HT plate reader (Biotek) at 550 nm, in a standard curve of sodium nitrite.

3.2.5 Western blotting

Total cell protein (25 μg) was denatured at 95 °C in sample buffer (5% SDS, 0.125 M Tris–HCl, pH 6.8, 20% glycerol, 10% 2-mercaptoethanol and bromophenol blue) for 5 min and separated by SDS-PAGE under reducing conditions. Proteins were electrotransferred onto

PVDF membranes using a wet transfer system at 350mA for 210 min. After blocking with 5% nonfat dry milk in Tris-buffered saline TBS-Tween 20 (0.1%) for 2 h, membranes were probed overnight at 4 °C with a rabbit monoclonal antibody, diluted at 1:1000, against Interleukin-1β (Abcam, Cambridge, UK) or with a mouse monoclonal anti-iNOS antibody (R&D Systems, Minneapolis, MN, USA), diluted at 1:500. Membranes were washed with TBS-Tween 20 and incubated with anti-rabbit or anti-mouse secondary antibodies, respectively, diluted at 1:5000 (Santa Cruz Biotechnology, Dallas, TX, USA). β-Tubulin was detected with a mouse monoclonal antibody diluted at 1:20000 (Sigma-Aldrich Co.) and was used as loading control. Immune complexes were detected with Clarity Western ECL Substrate (Bio-Rad Laboratories, Inc.) using the imaging system ImageQuant™ LAS 500 (GE Healthcare). Image analysis was performed with TotalLab TL120 software (Nonlinear Dynamics Ltd., Newcastle upon Tyne, UK).

3.2.6 Statistical analysis

Results are presented as means ± SEM. Statistical analysis was performed using GraphPad Prism version 8.0.2 (GraphPad Software, San Diego, CA, USA). Statistical significance was evaluated with one-way ANOVA with the Dunnet post-test for comparison of multiple conditions or with the t-test to compare two distinct conditions. The results were considered statistically significant at $p<0.05$.

4. Results

4.1 Semi-synthesis of CIAD7 derivatives

4.1.1 Acid-catalyzed hydration

Alcohols formation by acid-catalyzed addition of water to alkenes is an essential reaction in organic chemistry and it can be regarded as involving a carbocation intermediate. The alkene is protonated and then reacts with water. This mechanism explains the formation of the more highly substituted alcohol from unsymmetrical alkenes, following the Markovnikov's rule (Carey and Sundberg, 2007).

Alkenes do not react with pure water, as water is not acidic enough to allow hydrogen to act as an electrophile to start a reaction. However, in the presence of a small amount of an acid, the reaction does occur, resulting in an alcohol. The most commonly used acid to catalyze this reaction is H_2SO_4 in an aqueous solution (Liu, Xin).

Figures 4 and 5 represent the synthesis of GM1 and GM2, respectively, starting from CIAD7.

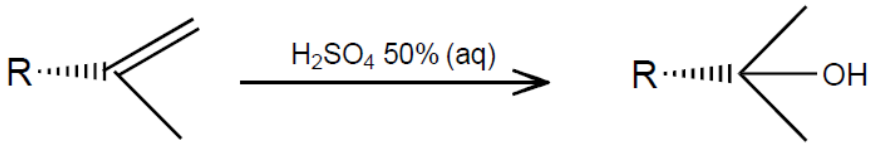

Figure 4. Synthesis of GM1 starting from R-(-)-CIAD7.

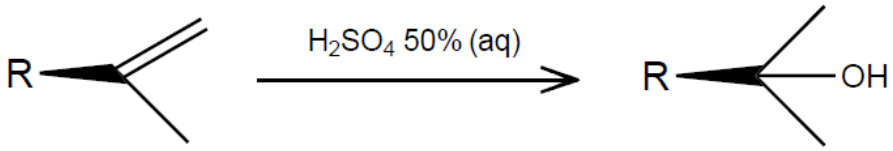

Figure 5. Synthesis of GM2 starting from S-(+)-CIAD7.

The original compound was mixed with an aqueous solution of H_2SO_4 in an ice bath for 24 h (TLC control). After extracting the final compound, it was purified by flash chromatography.

Partial NMR spectra (^{1}H, ^{13}C and DEPT 135) are shown below in Figures 6 and 7.

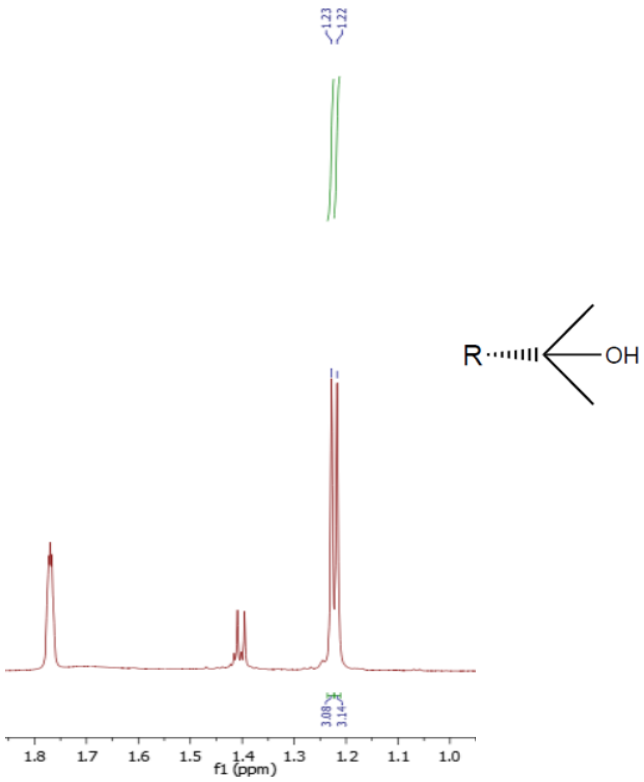

Figure 6. Partial ^{1}H NMR spectrum of GM1.

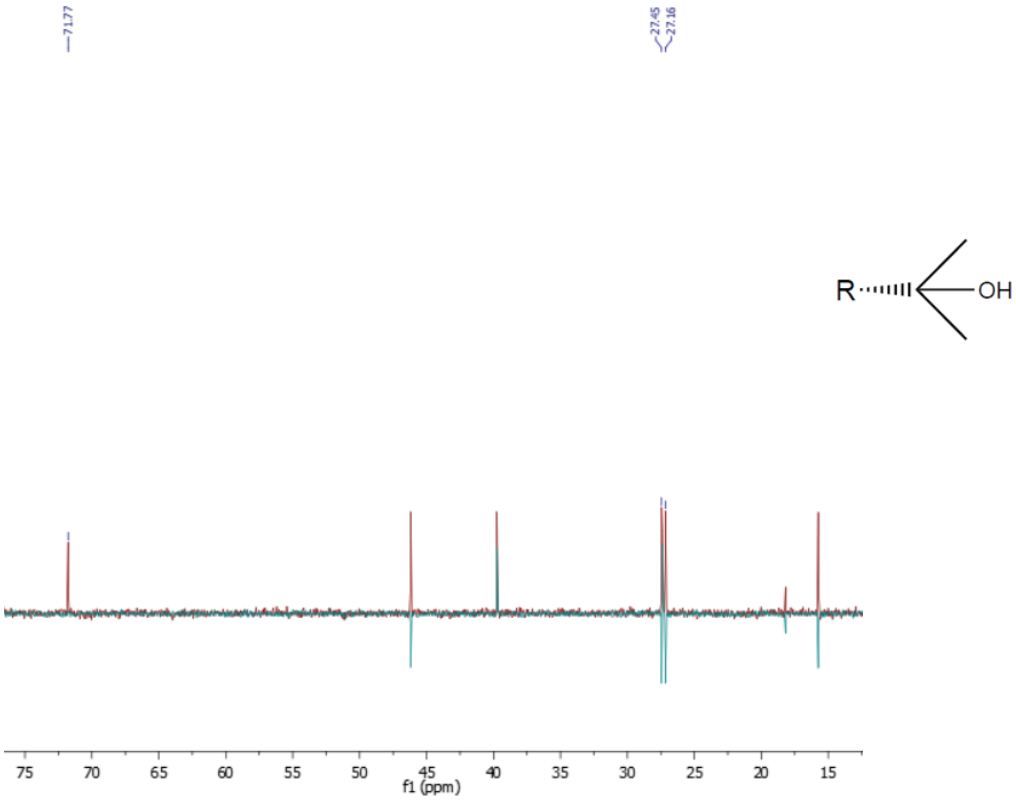

Figure 7. Partial ^{1}C NMR and DEPT 135 spectra of GM1.

We can assume that both ^{1}H NMR and ^{13}C NMR spectra of GM2 will be similar to those of GM1 since these two compounds are enantiomers. The corresponding nuclei in both enantiomeric environments have the same electronic surrounding, resulting in the same chemical shift.

GM1 is characterized by the presence two signals that appear as a singlet (s) in ^{1}H NMR spectrum, at δ 1.22 and 1.23 ppm. These signals correspond to the two methyl groups attached to the quaternary carbon (-C$\underline{H}_3$).

In ^{13}C NMR partial spectrum of GM1, we identified at δ 71.77 ppm the quaternary carbon of the alcohol group (-$\underline{C}$OH), and signals at δ 27.45 and 27.16 correspond to the two methyl groups (-$\underline{C}H_3$).

The association of DEPT (Distortionless Enhancement by Polarization Transfer) 135 with ^{13}C NMR spectroscopy is a big advantage to spectra analysis, as it can fully separate the carbon signals. DEPT 135 allows the distinction between CH and CH_3 from CH_2 by the phase of the signals (Chamberlain, 2013).

Partial FT-IR spectrum of GM1 is shown below in Figure 8.

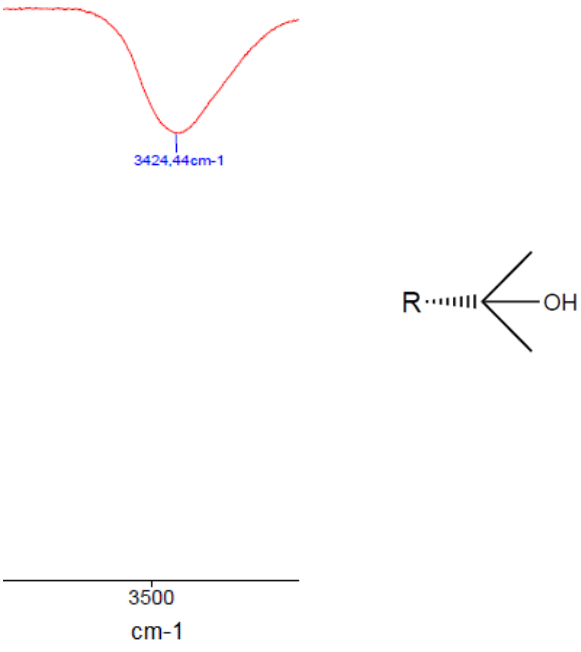

Figure 8. Partial FT-IR spectrum of GM1.

In the partial FT-IR spectrum, the band of the elongation of the O-H bond of the alcohol group is highlighted at 3424 cm^{-1}.

4.1.2 Esterification of tertiary alcohols

The conversion of alcohols to esters by O-acylation is a very important reaction in organic chemistry. Acyl halides and acid anhydrides react rapidly with most unhindered alcohols to generate esters in the presence of a catalyst. These two are very reactive acylating reagents because of a combination of the polar effect of the halogen or oxygen substituent, which enhances the reactivity of the carbonyl group, and the ease with which they can expel relatively good leaving groups (Carey and Sundberg, 2007). The catalyst that is often used is pyridine. However, DMAP has been recognized as a way more effective catalyst for the acylation of secondary or tertiary alcohols in the presence of acid anhydride, comparing to pyridine (Mandai *et al.*, 2016).

Figures 9 and 10 represent the synthesis of GM22 and GM23, starting from GM2 and GM1, respectively.

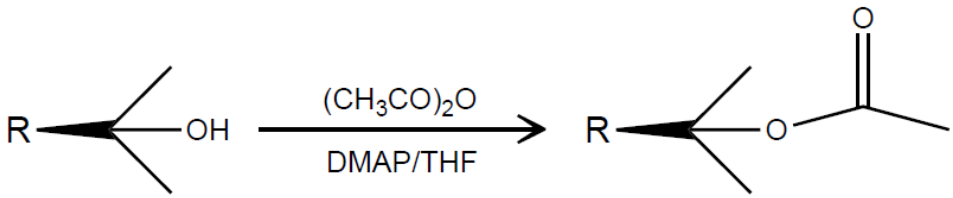

Figure 9. Synthesis of GM22 starting from GM2.

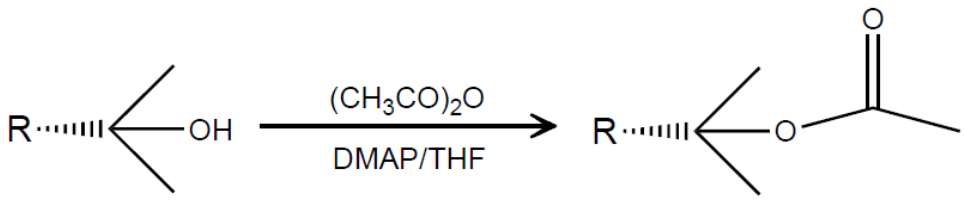

Figure 10. Synthesis of GM23 starting from GM1.

This synthetic procedure was adapted from (Figueiredo *et al.*, 2017). The substrate was dissolved in THF. Afterwards, the reagent (acid anhydride) and the catalyst (DMAP) were added into the mixture and it was kept stirring overnight at room temperature (TLC control). The final product was then purified by flash chromatography.

Partial ^{1}H NMR and complete ^{13}C and DEPT 135 spectra are shown below in Figures 11 and 12. We can assume that ^{1}H NMR, ^{13}C NMR and DEPT 135 spectra of GM23 will be similar to those of GM22 since these products are enantiomers, so both products will present specters with the same chemical shifts.

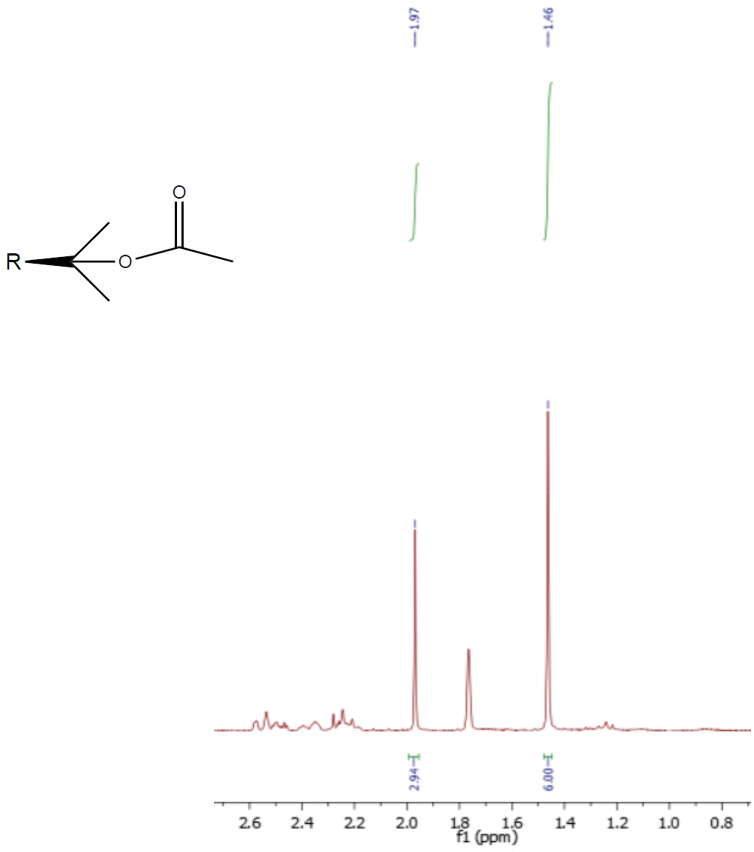

Figure 11. Partial ^{1}H NMR spectrum of GM22.

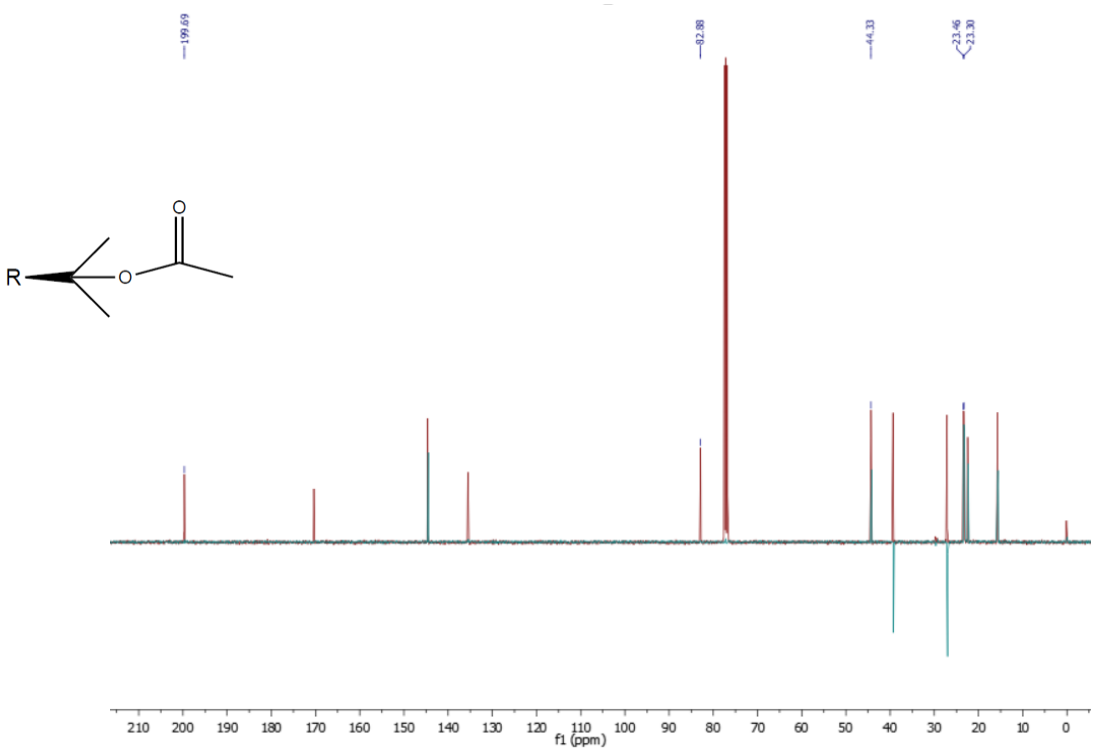

Figure 12. ^{13}C NMR and DEPT 135 spectra of GM22.

GM22 is characterized by the presence of a signal that appears as a singlet (s) in ^{1}H NMR spectrum at δ 1.97 ppm. This signal corresponds to the 6 hydrogens of the 2 methyl groups (-C<u>H</u>$_3$). These two methyl groups appear as a singlet in the ^{1}H NMR spectrum because they present the same chemical environment. GM22 also is also characterized by the presence of another singlet (s) at δ 1.46 ppm, that corresponds to the methyl in the ester group (-OCOC<u>H</u>$_3$).

In ^{13}C NMR and DEPT 135 partial spectra of GM22, we identified at δ 199.69 ppm the carbonyl carbon of the ester group of the compound (-O<u>C</u>OCH$_3$). The signal at δ 44.33 ppm corresponds to the methyl group of the ester (-OCO<u>C</u>H$_3$), and signals at δ 23.30 ppm and δ 23.46 ppm correspond to the primary carbons of the two other methyl groups (-<u>C</u>H$_3$).

Partial FT-IR spectrum of GM22 is shown in Figure 13.

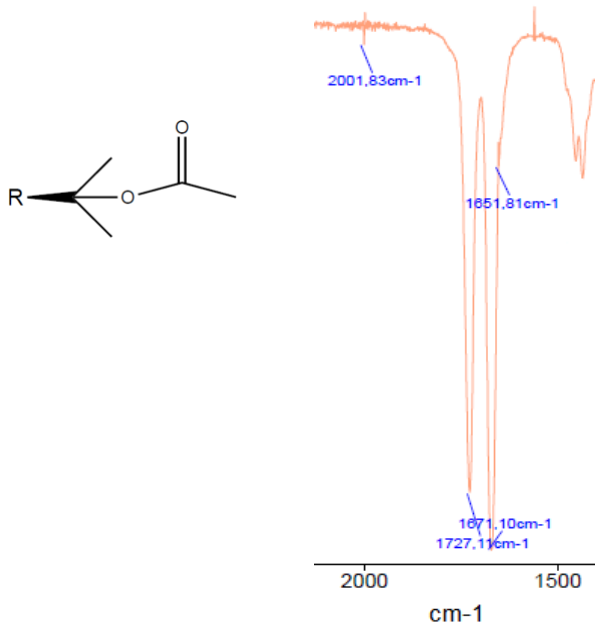

Figure 13. Partial FT-IR spectrum of GM22.

In the partial FT-IR spectrum, the band of the elongation of the C=O bond of the carbonyl ester is represented at 1727 cm^{-1}.

4.1.3 Epoxidation of alkenes

Converting alkenes into epoxides is a very useful transformation in organic synthesis. Epoxides are extremely valuable synthetic intermediates due to the high reactivity of the strained oxirane ring. The selectivity of the epoxidation reactions can be controlled by choosing appropriate reagents. One of the most useful reagents to perform the epoxidation of several different compounds is m-CPBA. This electrophilic reagent leads to the epoxide in a stereospecific manner. The reaction is thought to proceed *via* a single step that involves the nucleophilic attack of the alkene π-electrons onto the peroxy acid. For the epoxidation of electron-poor alkenes, the use of a nucleophilic oxidant such as hydrogen peroxide (H_2O_2) in an alkaline solution is able to generate α,β-epoxyketones with good yield. On the other hand, peroxy acids work well with electron-rich alkenes (Garcia, 2005).

The epoxidation of CIAD7 with m-CPBA is represented in Figures 14 and 15. GM3 was synthetized using R-(-)-CIAD7 as substrate and GM4 was obtained using S-(+)-CIAD7.

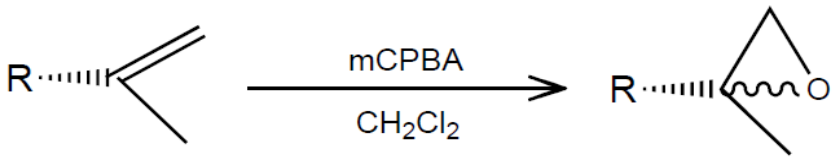

Figure 14. Synthesis of GM3 starting from R-(-)-CIAD7.

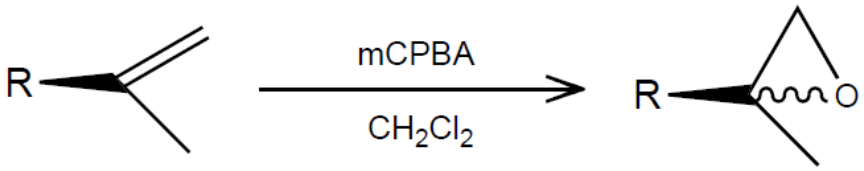

Figure 15. Synthesis of GM4 starting from S-(+)-CIAD7.

The synthetic procedure was adapted from (Eckrich *et al.*, 1996). The substrate was dissolved in ice-cold CH_2Cl_2, and m-CPBA was added dropwise for 10 min. The reaction was performed at 0 °C for 16 h (TLC control) and, after the work-up, the product obtained was purified via flash chromatography.

Partial NMR spectra (^1H, ^{13}C and DEPT 135) are shown below in Figures 16 and 17.

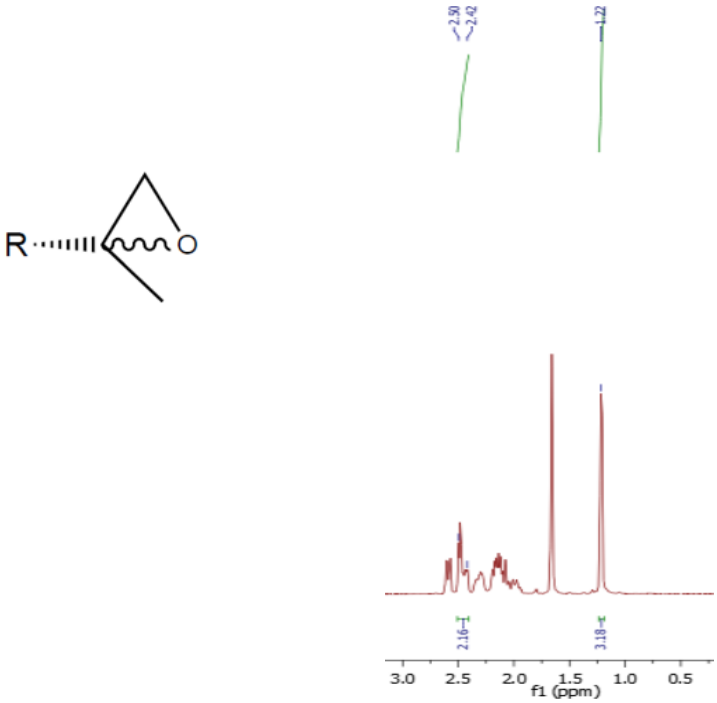

Figure 16. Partial ^1H NMR spectrum of GM3.

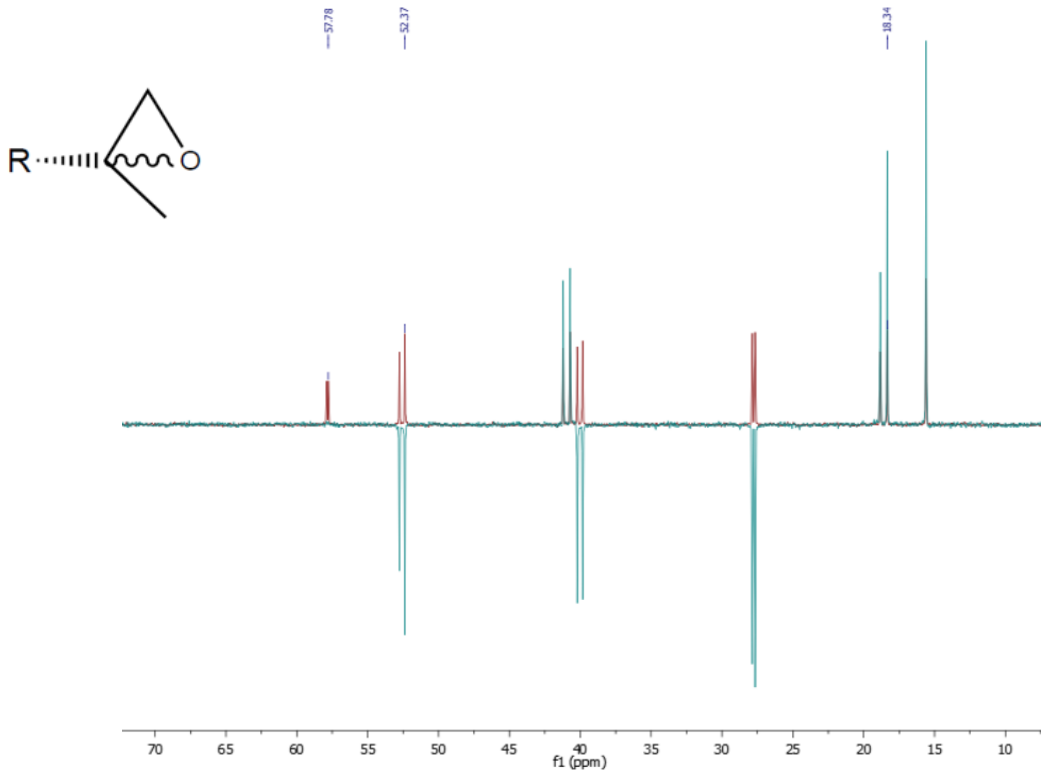

Figure 17. Partial ^{13}C NMR and DEPT 135 spectra of GM3.

The ^{1}H NMR spectrum of GM3 shows a multiplet (m) at δ 2.42 – 2.50 ppm, that corresponds to the two hydrogens of the oxirane ring (-C$\underline{H}_2$O) and a singlet (s) at δ 1.22 ppm, that corresponds to the methyl group (-C$\underline{H}_3$).

In ^{13}C NMR and DEPT 135 partial spectra of GM3, we noted at δ 57.78 ppm the quaternary carbon of the compound (-$\underline{C}$). The signal at δ 52.37 ppm corresponds to the secondary carbon of the oxirane ring (-$\underline{C}H_2$O), and signal δ 18.32 ppm corresponds to the primary carbon of the methyl group (-$\underline{C}H_3$).

Partial FT-IR spectra of GM3 is shown in Figure 18.

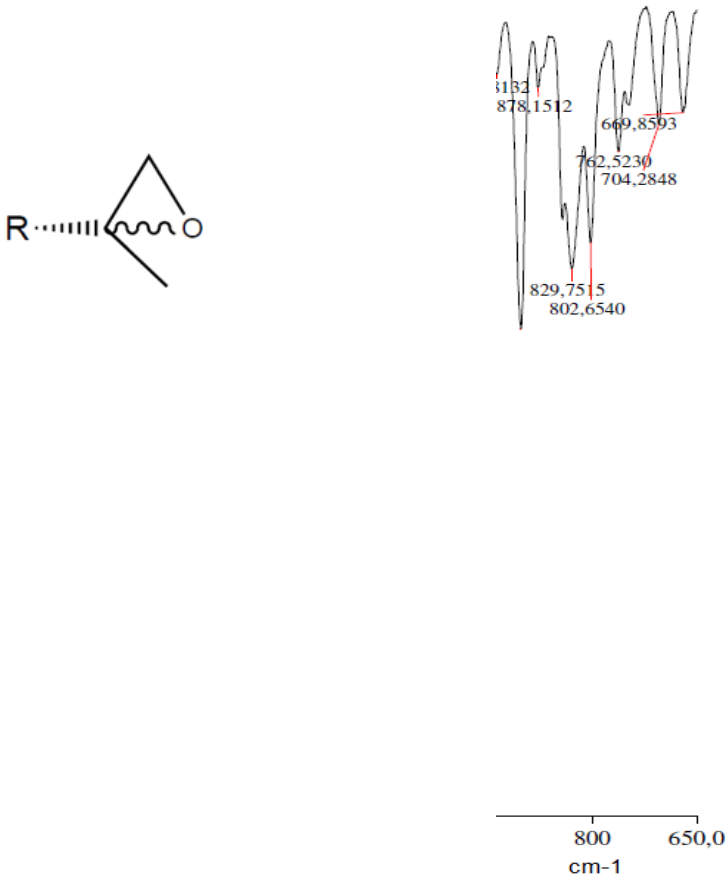

Figure 18. Partial FT-IR spectrum of GM23.

In the partial FT-IR spectrum, the bands of the C-O bond elongation of the epoxide group are represented at 802 and 829 cm^{-1}.

4.1.4 Nucleophilic ring-opening of epoxides

Ring opening of epoxides with nucleophilic reagents is a powerful tool for the preparation of various 1,2-disubstituted products. A simple protocol for the synthesis of β-alkoxy alcohols is the ring opening of epoxides with an appropriate alcohol under acidic or basic conditions (Leitão *et al.*, 2008).

Leitão *et al.,* (2008) showed that $NH_2NH_2.H_2SO_4$ can be used as an efficient catalyst for the synthesis of β-alkoxy alcohols at room temperature. Based on this information, we synthetized 8 compounds and their respective diastereoisomers, using 2 different primary alcohols: MeOH and EtOH as nucleophilic agents and solvents (Figures 19 to 22).

A. Nucleophilic ring-opening of epoxides in the presence of MeOH

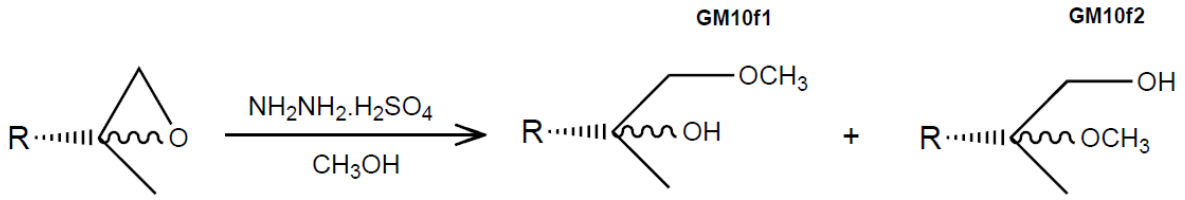

Figure 19. Synthesis of GM10f1 and GM10f2 starting from GM3.

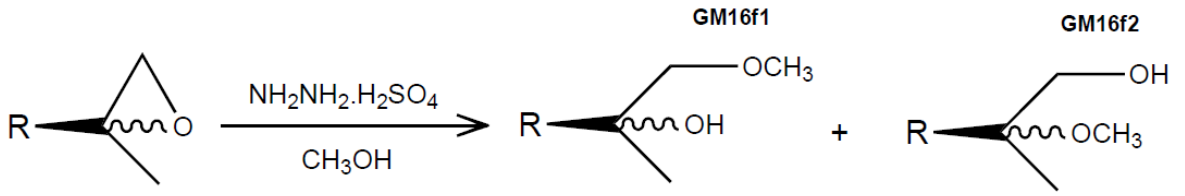

Figure 20. Synthesis of GM16f1 and GM16f2 starting from GM4.

B. Nucleophilic ring-opening of epoxides in the presence of EtOH

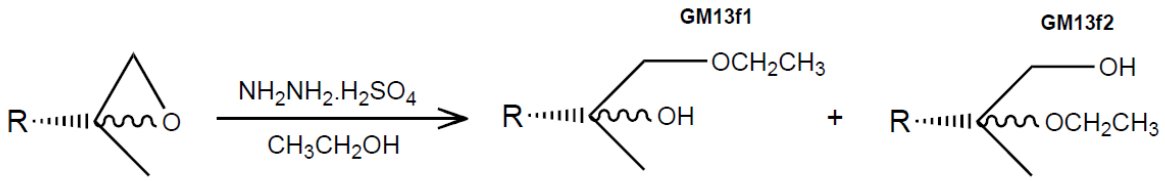

Figure 21. Synthesis of GM13f1 and GM13f2 starting from GM3.

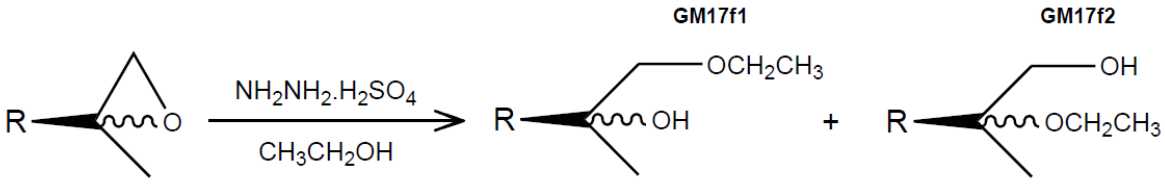

Figure 22. Synthesis of GM17f1 and GM17f2 starting from GM4.

GM3 (or GM4) was dissolved in MeOH or EtOH and $NH_2NH_2.H_2SO_4$ was added into the mixture. Initially, we performed the reactions at room temperature as described by Leitão *et al.*, but without successful results. Therefore, we decided to perform the reactions under reflux. The final products were then purified by flash chromatography.

Partial NMR spectra (^1H, ^{13}C and DEPT 135) allows us to affirm that for each reaction, the result is a mixture of two diastereoisomers (1:1). Figures 23 to 28 show the spectra of the different compounds mentioned above.

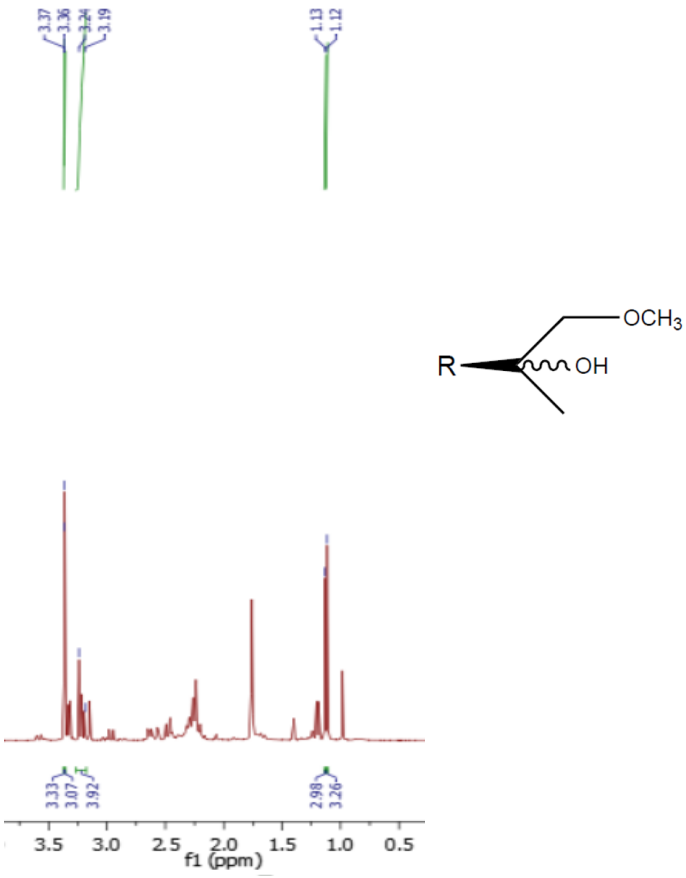

Figure 23. Partial ^1H NMR spectrum of GM16f1.

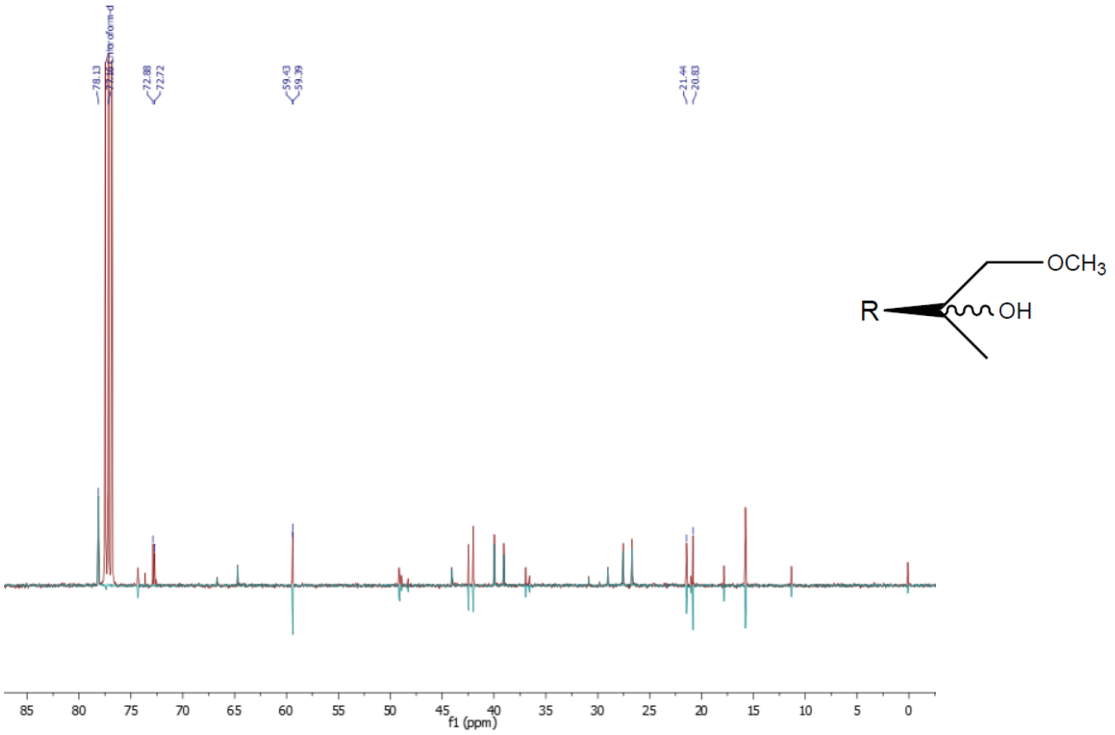

Figure 24. Partial ^{13}C NMR and DEPT 135 spectra of GM16f1.

Again, since GM10f1 and GM16f1 are enantiomers, we assume that ^{1}H NMR, ^{13}C NMR and DEPT 135 spectra of GM16f1 are similar to those of GM10f1, hence why we do not present the spectra for GM10f1.

GM16f1 is characterized by the presence of a signal that appears as a multiplet (m) in ^{1}H NMR spectrum, between δ 3.19 – 3.24 ppm. This signal represents 2 hydrogens of the methylene group (-C$\underline{H}_2$OH). At δ 3.36 [3.37] ppm, we identified a singlet signal that corresponds to the 3 hydrogens of the methoxy group (-OC$\underline{H}_3$) and at δ 1.12 [1.13] ppm there is a singlet that represents 3 hydrogens from the methyl group (-C$\underline{H}_3$). The values in square brackets represent GM16f1's diastereoisomer.

In ^{13}C NMR partial spectrum of GM16f1, we identified at δ 78.13 [78.13] ppm the carbon that is bonded to the alcohol group (-$\underline{C}$H$_2$OH). At δ 72.72 [72.88] ppm, it is represented the quaternary carbon (-$\underline{C}$) and at δ 59.39 [59.43] ppm we identified the carbon of the methoxy group (-O$\underline{C}$H$_3$). Lastly, the signal at δ 20.83 [21.44] ppm corresponds to the methyl group attached to the quaternary carbon (-$\underline{C}$H$_3$). Again, the values in square brackets represent GM16f1's diastereoisomer.

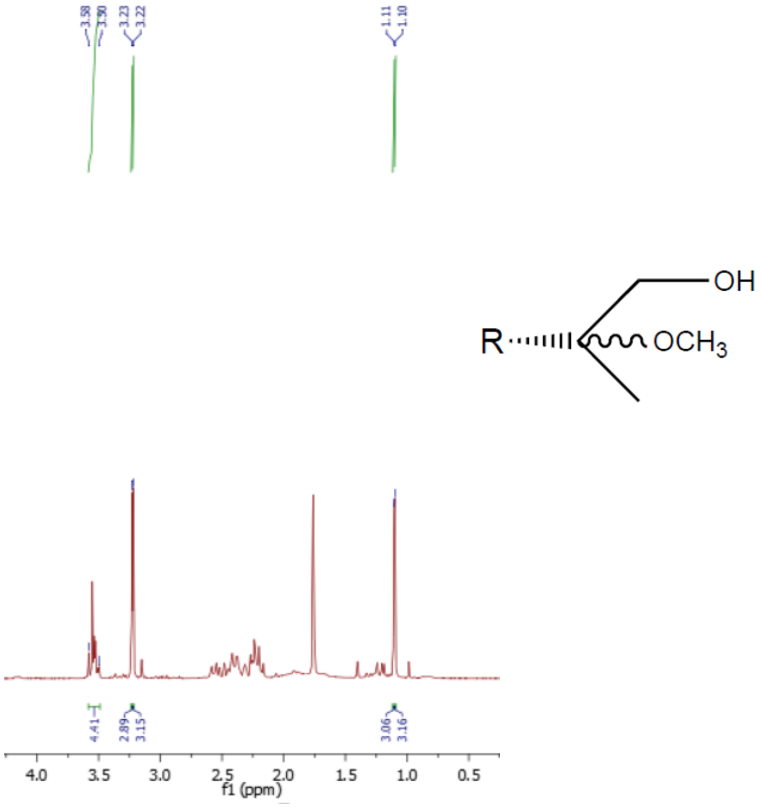

Figure 25. Partial ^{1}H NMR spectrum of GM10f2.

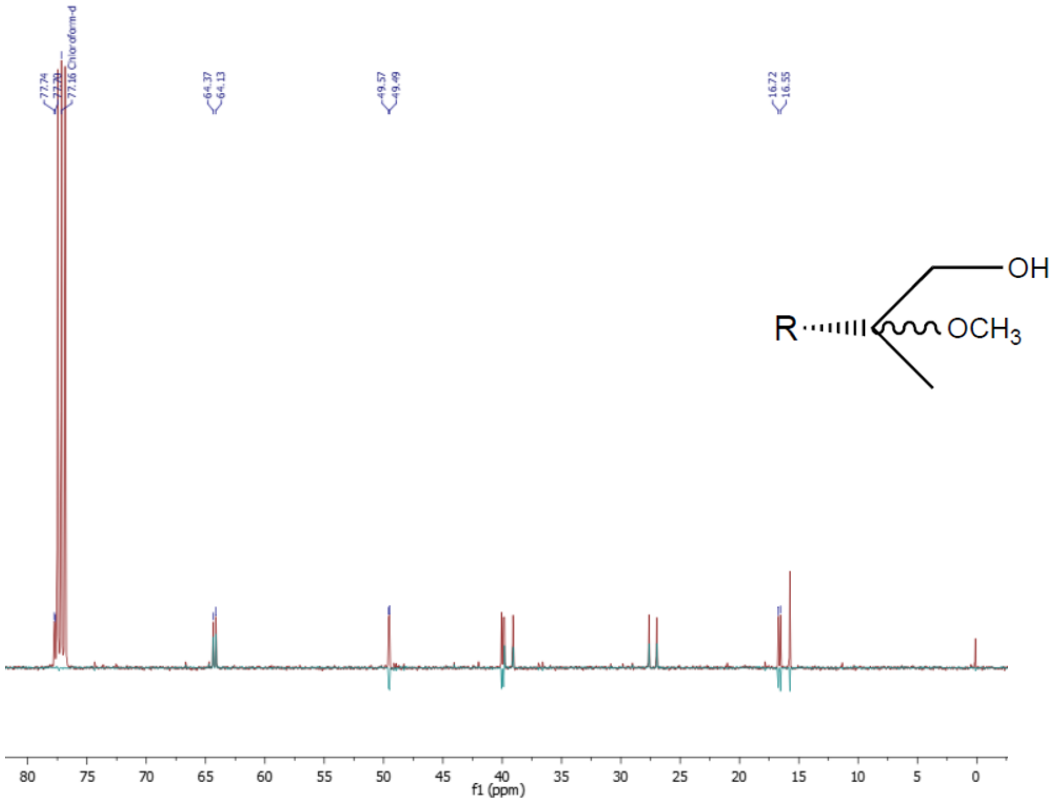

Figure 26. Partial ^{13}C NMR and DEPT 135 spectra of GM10f2.

GM10f2 is characterized by the presence of a multiplet (m) signal in ^{1}H NMR spectrum, between δ 3.50 – 3.58 ppm. This signal represents the 2 hydrogens of the methylene group (-C$\underline{H}_2$OH). At δ 3.22 [3.23] ppm, we identified a singlet signal that corresponds to the 3 hydrogens of the methyl group attached to another oxygen atom (-OC$\underline{H}_3$) and at δ 1.10 [1.11] ppm there is a singlet that represents 3 hydrogens from the methyl group bonded to the quaternary carbon (-C$\underline{H}_3$). The values in square brackets represent GM10f2's diastereoisomer.

In ^{13}C NMR partial spectrum of GM10f2, we identified at δ 77.70 [77.74] ppm the quaternary carbon (-$\underline{C}$). At δ 64.13 [64.37] ppm, it is represented the carbon attached to the alcohol group (-$\underline{C}$H$_2$OH) and at δ 49.49 [49.57] ppm we identified the carbon attached to the oxygen atom (-OC$\underline{H}_3$). Lastly, the signal at δ 16.55 [16.72] ppm corresponds to the methyl group attached to the quaternary carbon (-$\underline{C}$H$_3$). Again, the values in square brackets represent GM10f2's diastereoisomer.

Since GM10f2 and GM16f2 are enantiomers, we assume that ^{1}H NMR, ^{13}C NMR and DEPT 135 spectra of GM10f2 are similar to those of GM16f2, that is why we do not present the spectra for GM16f2.

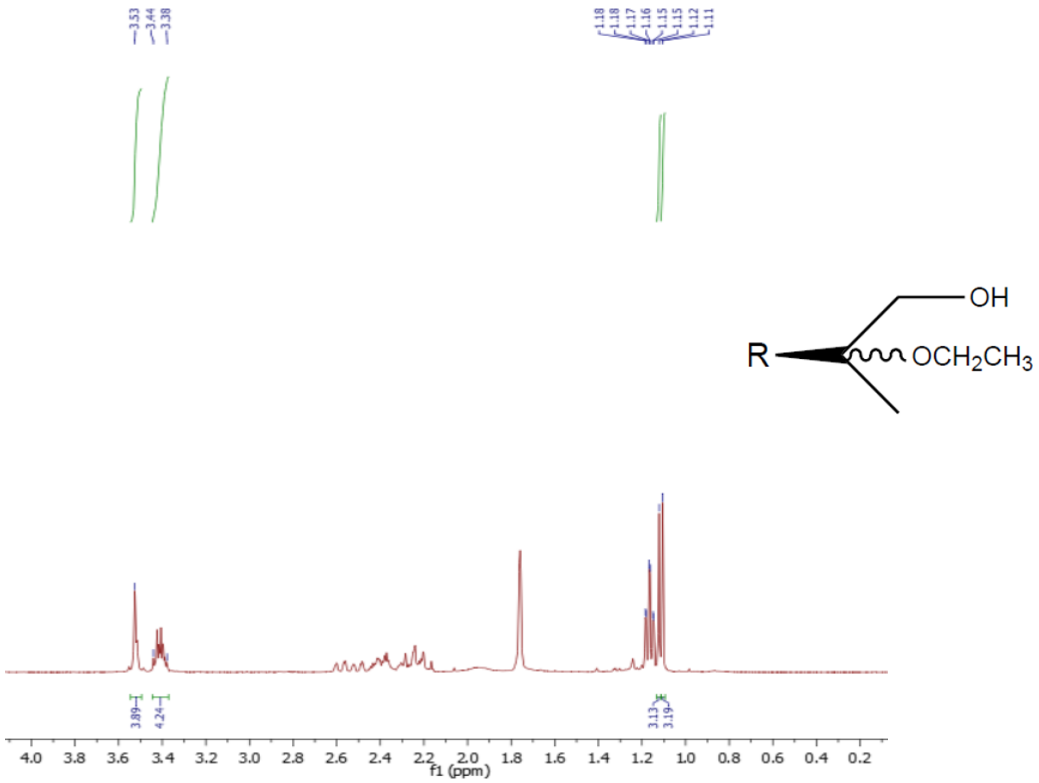

Figure 27. Partial ^{1}H NMR spectrum of GM17f2.

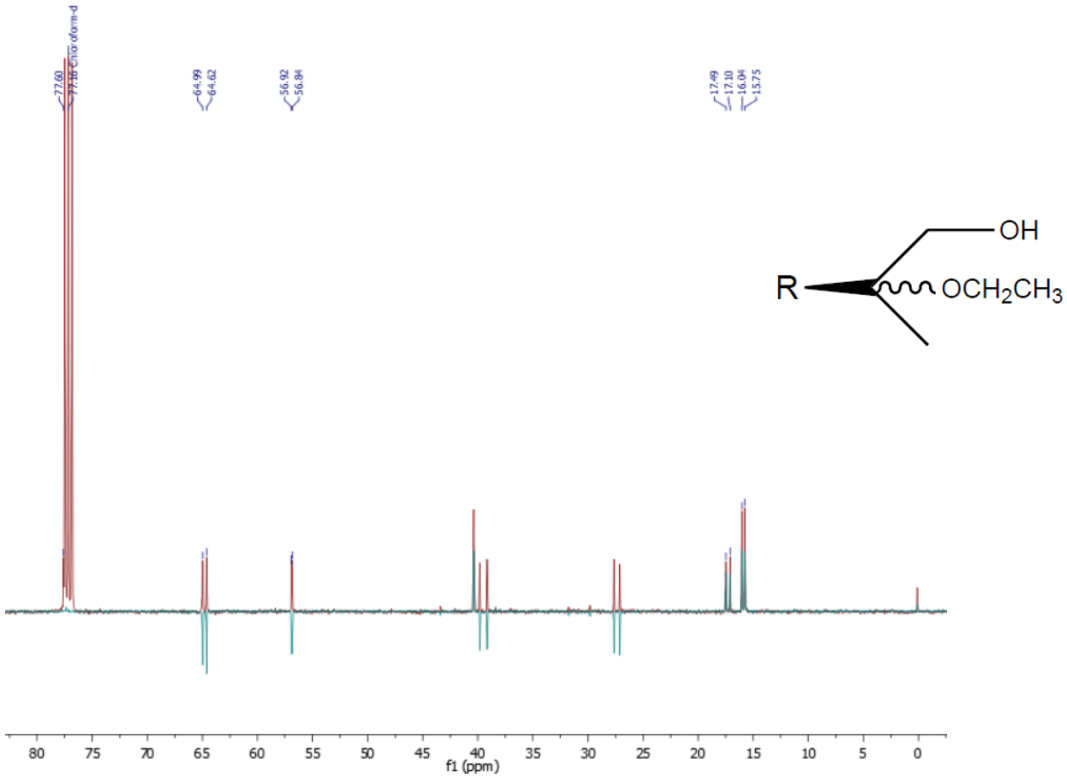

Figure 28. Partial ^{13}C NMR and DEPT 135 spectra of GM17f2.

As GM13f2 and GM17f2 are enantiomers, again we assume that ^{1}H-NMR, ^{13}C-NMR and DEPT-135 spectra of GM13f2 have to be similar to those of GM17f2, that is why we do not present any spectra for GM13f2.

GM17f2 is characterized by the presence of a singlet (s) signal in ^{1}H NMR spectrum, at δ 3.53 [3.53] ppm. This signal represents the methylene of the alcohol group (-OC<u>H</u>$_2$OH). Between δ 3.38 – 3.44 ppm, we identified a multiplet (m) signal that corresponds to the 2 hydrogens of the ether group (-OC<u>H</u>$_2$CH$_3$) and at δ 1.16 [1.17] ppm there is a triplet (t) signal, J = 6.0 Hz, that represents 3 hydrogens from the methyl group (-OCH$_2$C<u>H</u>$_3$). The values in square brackets represent GM17f2's diastereoisomer.

In ^{13}C NMR partial spectrum of GM17f2, we identified at δ 77.60 [77.60] ppm the quaternary carbon (-<u>C</u>). At δ 64.62 [64.99] ppm, it is represented the carbon attached to the hydroxyl group (-<u>C</u>H$_2$OH) and at δ 56.84 [56.92] ppm the secondary carbon of the ethoxy group (-O<u>C</u>H$_2$CH$_3$). Lastly, the signal at δ 17.10 [17.49] ppm corresponds to the methyl group attached to the quaternary carbon (-<u>C</u>H$_3$) and the signal at δ 15.75 [16.04] ppm represents the methyl group of the ethoxy (-OCH$_2$<u>C</u>H$_3$). Again, the values in square brackets represent GM17f2's diastereoisomer.

We could not present any spectra for GM13f1 and GM17f1 because both products presented considerable amounts of impurities after analyzing both ^{1}H NMR and ^{13}C NMR spectra.

Partial FT-IR spectra for GM16f1, GM10f2 and GM17f2 are shown below in Figures 29, 30 and 31.

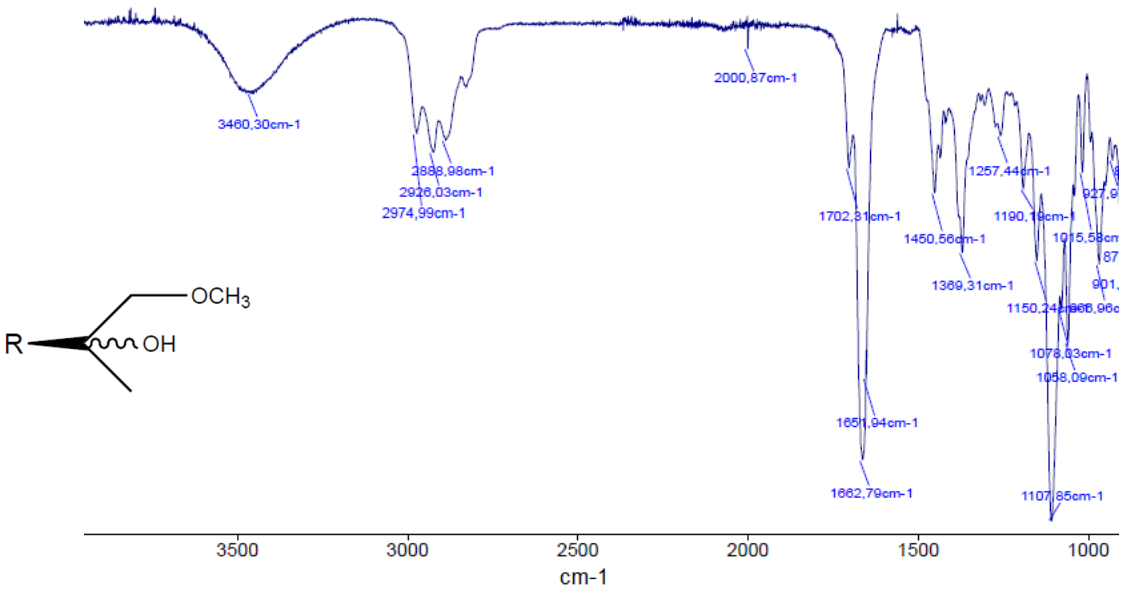

Figure 29. Partial FT-IR spectrum of GM16f1.

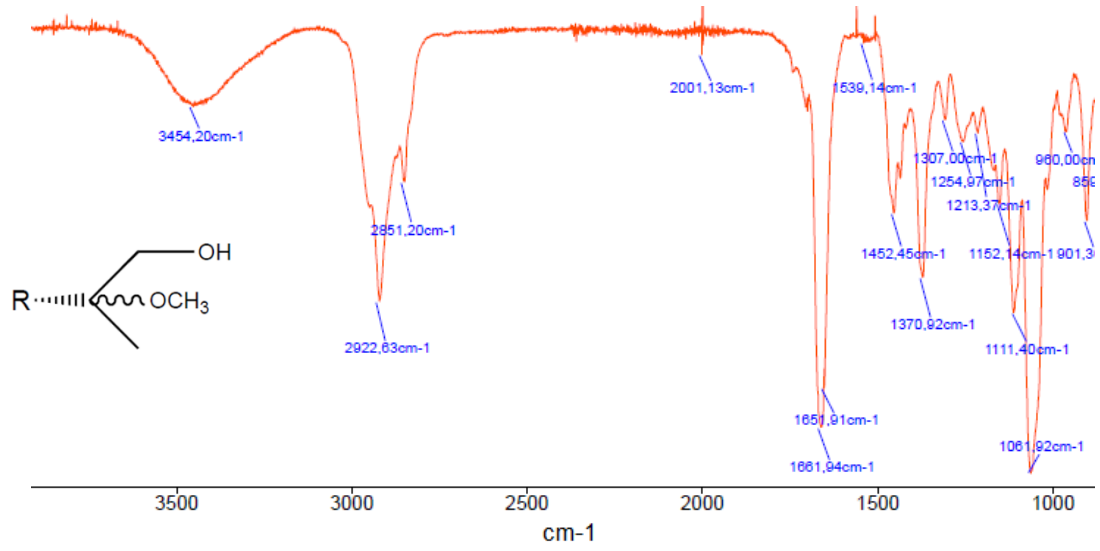

Figure 30. Partial FT-IR spectrum of GM10f2.

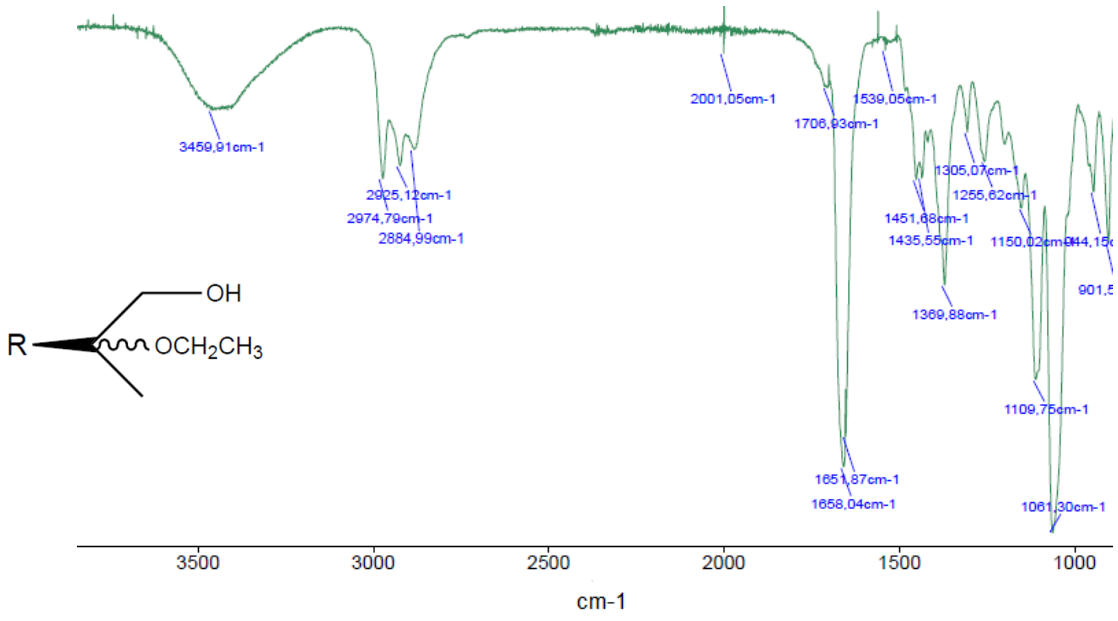

Figure 31. Partial FT-IR spectrum of GM17f2.

In the partial FT-IR spectrum of GM16f1 (Figure 29), we can identify the band of the elongation of the O-H bond at 3460 cm^{-1} and the elongation bands for C-O bonds at 1107 cm^{-1}. Figure 30 corresponds the partial FT-IR spectrum of GM10f2, were the band at 3454 cm^{-1} represents the elongation of the O-H bond and the band at 1061 cm^{-1} represents the elongation bands for the C-O bonds. Finally, in the partial FT-IR spectrum of GM17f2 (Figure 31), we can observe the band of the elongation of the O-H bond at 3459 cm^{-1} and the band that corresponds to the elongation of the C-O bonds is at 1061 cm^{-1}.

4.2 Pharmacological characterization of CIAD7 derivatives

4.2.1 GM2

4.2.1.1 Cell Viability of GM2-treated Raw 264.7 macrophages

Several concentrations of GM2 were first evaluated for cytotoxicity, in the absence or presence of LPS, using the resazurin reduction assay, which indirectly evaluates cell viability (Figure 32). Cytotoxicity was defined according to the standard for cytotoxicity assessment, ISO 10993-5, as the highest concentration that did not decrease cell viability by more than 30% relative to cells treated with LPS alone. Results in Fig. 32A show that in LPS-treated cells, none of the GM2 concentrations tested had cytotoxic effects. Although results for concentrations of 600, 900 and 1200 µM showed statistically significant increases in metabolic activity, the effect is very small and biologically irrelevant, probably due to increased mitochondrial activity. Fig. 32B represents cell viability results in cells treated with the vehicle alone. The highest GM2 concentration tested, 2400 µM, caused a statistically significant reduction of cell viability, but the remaining cell viability is still higher than 70%, thus above the limit for cytotoxicity defined in the standard for cytotoxicity assessment. Therefore, it can be concluded that in concentrations up to 2400 µM, GM2 has no cytotoxic effects in Raw 264.7 macrophages (Fig. 32B).

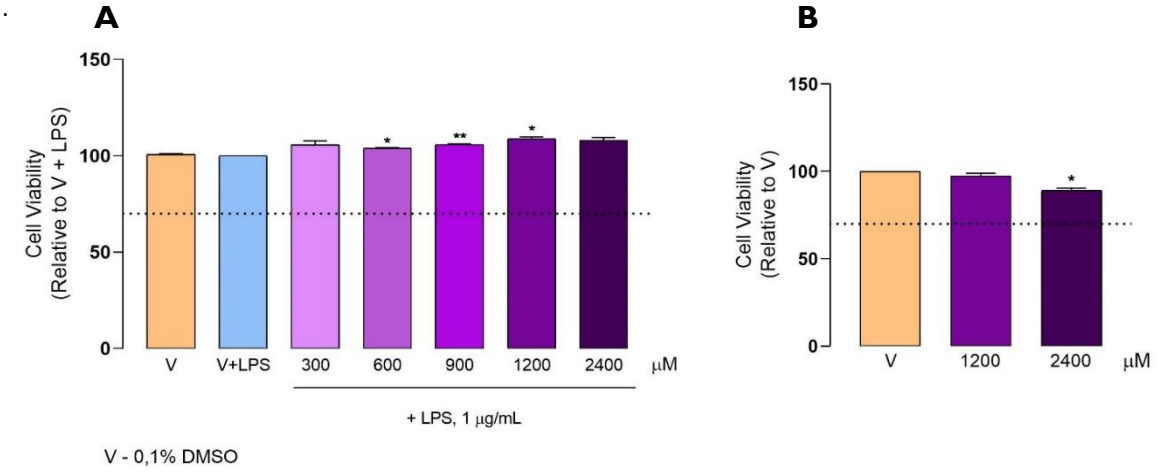

Figure 32. Effect of GM2 on cell viability. Raw 264.7 macrophage cultures were treated with the vehicle (0.1% DMSO) or the indicated concentrations of GM2, for 1 h before addition of 1 µg/mL LPS for 18 h. Control cells (V) were treated with the vehicle alone (0.1% DMSO) for the same period (**A**). Raw 264.7 macrophage cultures were treated with 1200 or 2400 µM GM2 for 18 h in the absence of LPS; control cells (V) were treated with the vehicle alone (0,1% DMSO) for the same period (**B**). Each column represents the mean ± SEM of three independent experiments. *p<0.05. **p<0.01 relative to LPS-treated cells (V+LPS). The dotted line represents the 70% cell viability mark that is accepted according to ISO 10993-5, as the lower limit for absence of cytotoxicity.

4.2.1.2 GM2 reduces LPS-induced NO production in Raw 264.7 macrophages

Since all the concentrations tested were found to be non-cytotoxic, they were all evaluated for the ability to inhibit LPS-induced NO production, which was assessed using the Griess assay (Figure 33). GM2 did not affect basal NO production when added to macrophage cultures in the absence of LPS (Fig. 33A). and it significantly reduced LPS-induced NO production in a concentration-dependent manner (Fig. 33B).

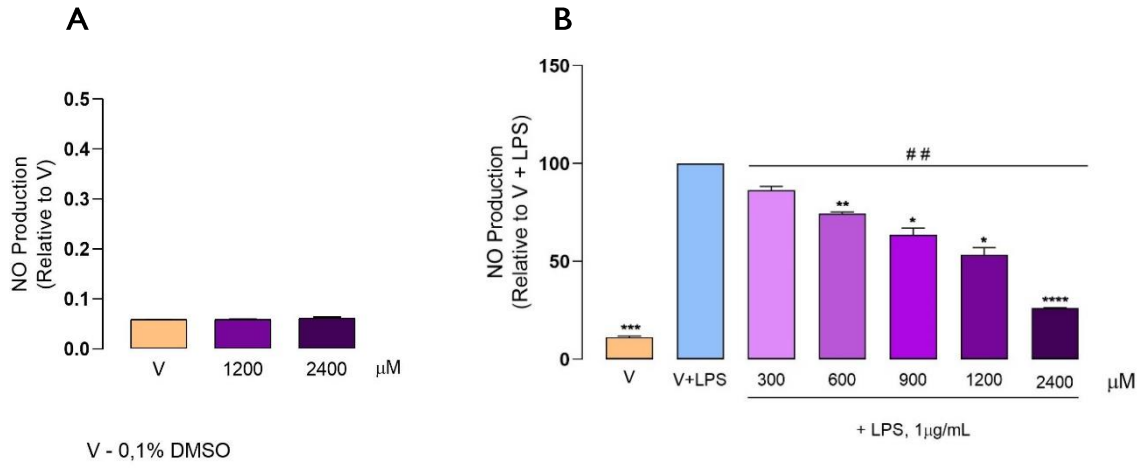

Figure 33. Effect of GM2 on NO production. Raw 264.7 cells were treated with 1200 or 2400 µM GM2 for 18 h in the absence of LPS; control cells (V) were treated with the vehicle alone (0,1% DMSO) for 18 h (**A**). Raw 264.7 macrophage cultures were treated with 1200 or 2400 µM GM2 for 18 h in the absence of LPS; control cells (V) were treated with the vehicle alone (0,1% DMSO) for the same period of time (**B**). Each column represents the mean ± SEM of three independent experiments. *p<0.05, **p<0.01, ***p<0.001 and ****p<0.0001 relative to LPS-treated cells (V+LPS). ##p < 0.01 relative to all the concentrations tested.

To evaluate GM2 potency, the concentration required to inhibit NO production by 50% (IC50) was determined mathematically, as shown in Figure 34.

The IC_{50} value obtained for GM2 is 1046 µM.

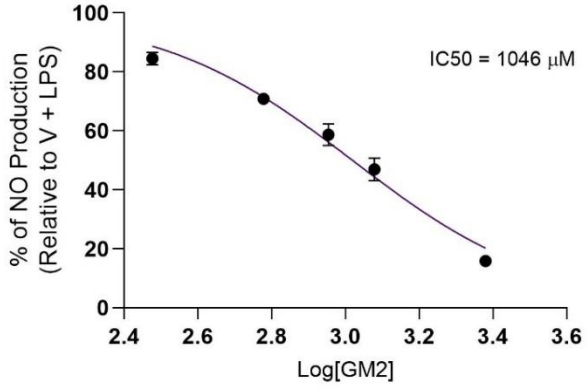

Figure 34. Concentration-response curve relative to inhibition of LPS-induced NO production by GM2 in the conditions depicted in Figure 33.

4.2.1.3 GM2 shows a tendency to inhibit LPS-induced iNOS expression on Raw 264.7 macrophages

To further confirm the anti-inflammatory properties of this compound, iNOS protein levels were evaluated by Western Blotting analysis. Treatment with 1 μg/mL LPS significantly increased iNOS protein levels in Raw 264.7 macrophages relative to cells treated with the vehicle alone (Figure 35). Treatment with GM2 decreased iNOS protein levels relative to cells treated with LPS alone, but the differences did not reach statistical significance, probably due to interassay variability and the small number of assays performed. However, at its highest concentration (2400 μM), GM2 completely prevented the increase in iNOS protein levels induced by LPS and the difference reached statistical significance.

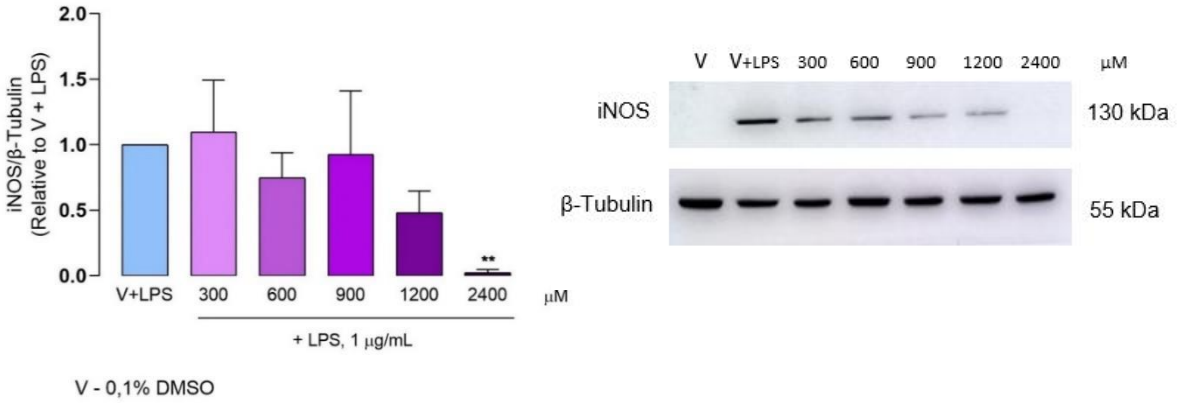

Figure 35. GM2 decreases LPS-induced iNOS protein levels in Raw 264.7 macrophages. Cells were treated with 1 μg/mL LPS for 18 h, following pre-treatment with the vehicle (0.1% DMSO) or GM2 concentrations indicated in the figure. Control cells (V) were treated with vehicle alone (0,1% DMSO) in the absence of LPS. Each column represents the mean ± SEM of three independent experiments. **p<0.01 relative to LPS-treated cells.

4.2.1.4 GM2 does not affect LPS-induced pro-IL-1β levels in Raw 264.7 macrophages

To further confirm anti-inflammatory properties of GM2, we evaluated its effect on the protein levels of pro-IL-1β, the unprocessed form of IL-1β. The results in Figure 36 show that the highest concentration nearly doubled pro-IL-1β levels, while the other concentrations had no detectable effect. However, the result did not reach statistical significance, probably due to the small number of assays that we could perform and the variability among them. Therefore, further studies must be performed to clearly identify the effect of GM2 on pro-IL-1β protein levels.

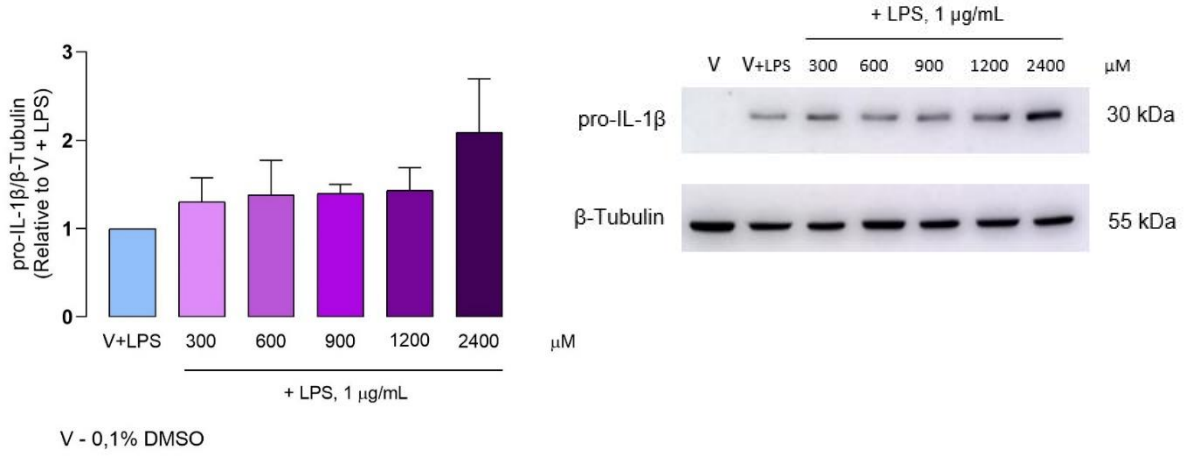

Figure 36. GM2 does not affect LPS-induced pro-IL-1β protein levels in Raw 264.7 macrophages. Cells were treated with 1 μg/mL LPS for 18 h, following pre-treatment with the vehicle (0,1% DMSO) or the concentrations of GM2 indicated. Control cells (V) were treated with vehicle alone (0,1% DMSO) in the absence of LPS. Each column represents the mean ± SEM of three independent experiments.

4.2.2 GM16f1

4.2.2.1 Cell viability of GM16f1-treated Raw 264.7 macrophages

Various concentrations of GM16f1 were evaluated for cytotoxicity, in the absence or presence of LPS, using the resazurin reduction assay, as shown in Figure 37. Again, cytotoxicity was defined according to the standard for cytotoxicity assessment, ISO 10993-5, as the highest concentration that did not decrease cell viability by more than 30% relative to cells treated with LPS alone. Results in Fig. 37A show that in LPS-treated cells, none of the GM16f1 concentrations tested had cytotoxic effects. Although results for the concentration of 300 μM have shown to be statistically significant, the difference relative to LPS-treated cells is very small and has no biological relevance. Fig. 37B represents cell viability results in cells treated

with the vehicle alone. The highest GM16f1 concentration (2400 µM) was found to be cytotoxic in the absence of LPS, as it decreased cell viability by more than 30%, even if the results were not considered statistically significant. Nonetheless, since the effect disappears in the presence of LPS, this result was not taken in consideration in further experiments.

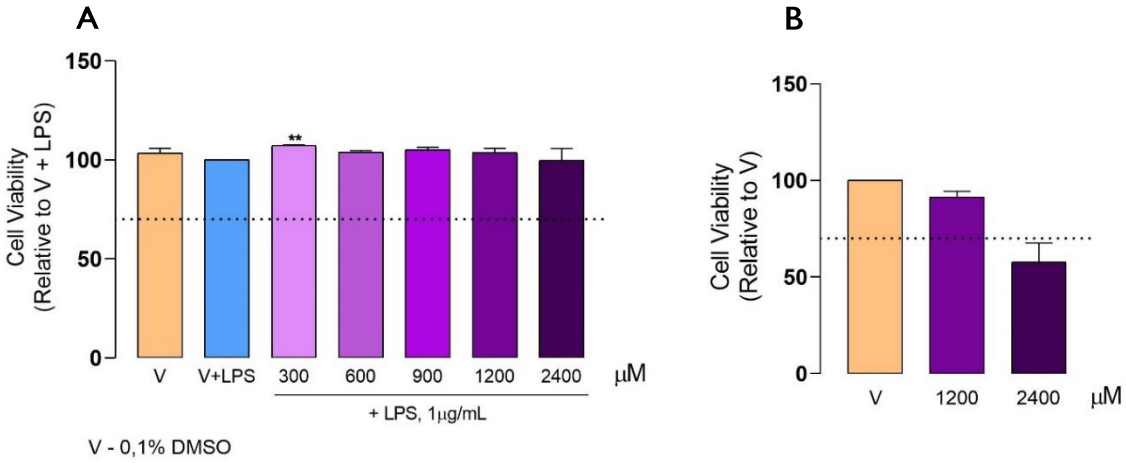

Figure 37. Effect of GM16f1 on cell viability. Raw 264.7 macrophage cultures were treated with the vehicle (0,1% DMSO) or the concentrations of GM16f1 indicated, for 1 h, before addition of 1 µg/mL LPS for 18 h. Control cells (V) were treated with the vehicle alone (0.1% DMSO) for the same period (**A**). Raw 264.7 macrophage cultures were treated with 1200 and 2400 µM C22 for 18 h in the absence of LPS; control cells (V) were treated with the vehicle alone (0,1% DMSO) for the same period (**B**). Each column represents the mean ± SEM of three independent experiments. **p<0.01 relative to LPS-treated cells (V+LPS). The dotted line represents the 70% cell viability mark that is accepted, according to ISO 10993-5, as the lower limit for absence of cytotoxicity.

4.2.2.2 GM16f1 reduces LPS-induced NO production in Raw 264.7 macrophages

At non-cytotoxic concentrations as observed in Figure 38, GM16f1 did not affect basal NO production when added to macrophage cultures in the absence of LPS (Fig. 38A), and it had a statistically significant effect on LPS-induced NO production. Results show that GM16f1 is able to reduce LPS-induced NO production in a concentration-dependent manner (Fig. 38B).

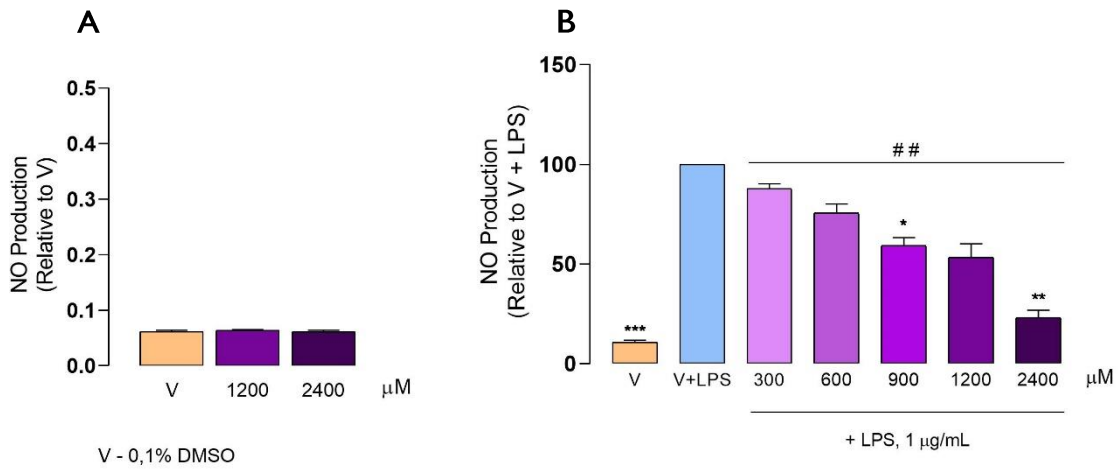

Figure 38. Effect of GM16f1 on NO production. Raw 264.7 macrophage cultures were treated with 1200 and 2400 µM GM16f1 for 18 h in the absence of LPS; control cells (V) were treated with the vehicle alone (0,1% DMSO) for the same period (**A**). Raw 264.7 macrophage cultures were treated with the vehicle (0.1% DMSO) or the concentrations of GM16f1 indicated, for 1 h before addition of 1 µg/mL LPS, for 18 h. Control cells (V) were treated with the vehicle alone (0.1% DMSO) for the same period (**B**). Each column represents the mean ± SEM. *p<0.05, **p<0.01 and ***p<0.001 relative to LPS-treated cells (V+LPS). ##p<0.01 relative to all the concentrations tested.

To evaluate GM16f1 potency, the concentration required to inhibit NO production by 50% (IC50) was determined as shown in Figure 39.

The IC_{50} value obtained for GM16f1 is 1010 µM.

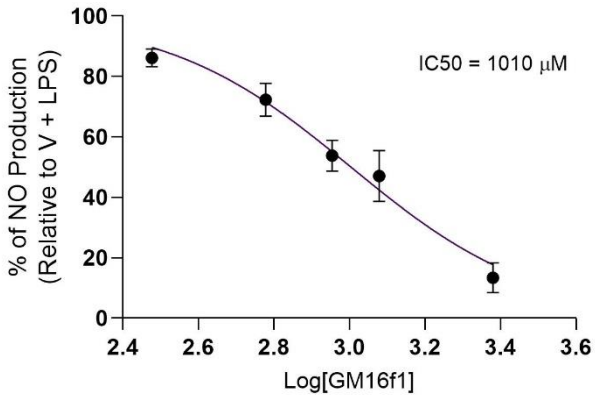

Figure 39. Concentration-response curve relative to inhibition of LPS-induced NO production by GM16f1 in the conditions depicted in Figure 38.

4.2.2.3 GM16f1 inhibits LPS-induced iNOS expression in Raw 264.7 macrophages

To further confirm the anti-inflammatory properties of GM16f1, iNOS protein levels were evaluated by Western Blotting analysis. Treatment with 1 μg/mL LPS significantly increased iNOS protein levels in Raw 264.7 macrophages relative to cells treated with the vehicle alone (Figure 40). Treatment with GM16f1 decreased iNOS protein levels relative to cells treated with LPS alone, and the reduction reached statistical significance at the two highest concentrations (1200 and 2400 μM).

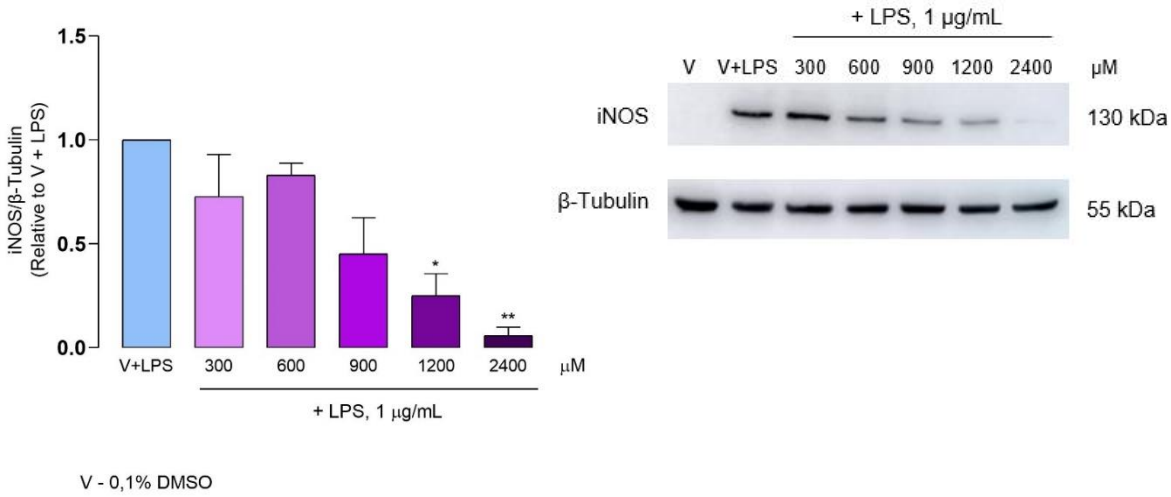

Figure 40. GM16f1 decreases LPS-induced iNOS protein levels in Raw 264.7 macrophages. Cells were treated with 1 μg/mL LPS for 18 h, following pre-treatment with vehicle (0.1% DMSO) or the GM16f1 concentrations indicated. Control cells (V) were treated with vehicle alone (0,1% DMSO) in the absence of LPS. Each column represents the mean ± SEM of three independent experiments. *$p<0.05$ and **$p<0.01$ relative to LPS-treated cells.

4.2.2.4 Effect of GM16f1 on LPS-induced pro-IL-1β levels in Raw 264.7 macrophages

As for GM2, the effect of GM16f1 on the protein levels of pro-IL-1β was evaluated. The results in Figure 41 show that GM2 at concentrations of 900 and 1200 μM greatly increased pro-IL-1β levels, but the results did not reach statistical significance, probably due to the small number of assays that we could perform and the variability among them. However, the highest concentration, 2400 μM, caused a slight decreased of pro-IL-1β protein levels that

due to very little variability among assays, reached statistical significance. Further studies will be required to fully assess the effect of GM16f1 on pro-IL-1β levels.

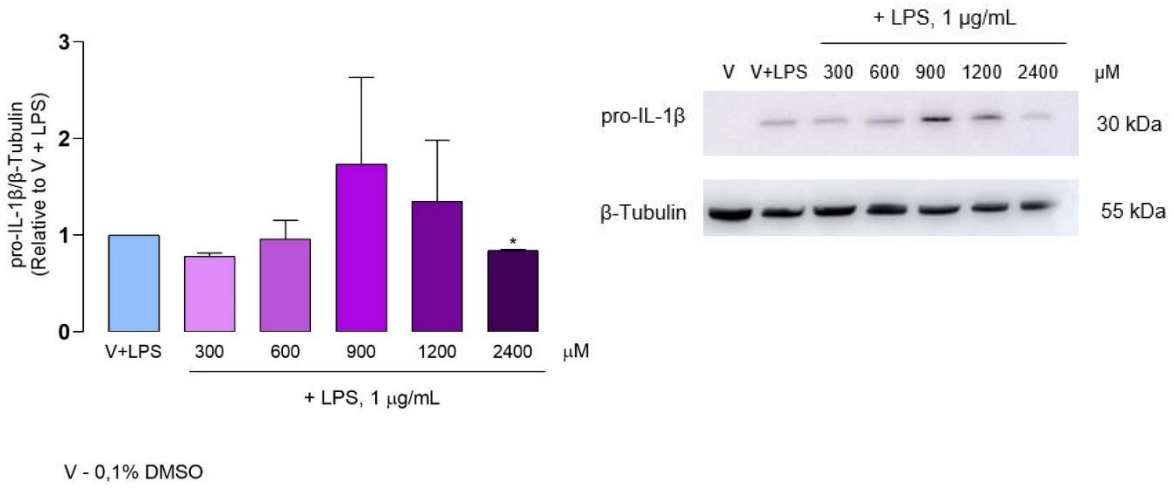

Figure 41. Effect of GM16f1 on LPS-induced pro-IL-1β protein levels in Raw 264.7 macrophages. Cells were treated with 1 μg/mL LPS for 18 h, following pre-treatment with vehicle (0.1% DMSO) or the concentrations of GM16f1 indicated. Control cells (V) were treated with vehicle alone (0.1% DMSO) in the absence of LPS. Each column represents the mean ± SEM of three independent experiments. *p<0.05 relative to LPS-treated cells.

4.2.3 GM22

4.2.3.1 Cell viability of GM22-treated Raw 264.7 macrophages

At a concentration of 2400 μM, GM22 was not completely miscible with the aqueous medium, due to its lipophilicity. Thus, this concentration was not tested. Results in Fig. 42A show that in LPS-treated cells, none of the GM22 concentrations tested is cytotoxic. The concentration of 600 μM caused a small, but statistically significant increase in resazurin reduction that has no biological significance. Results in Fig. 42B show that the highest concentration, 1200 μM, was cytotoxic in the absence of LPS as it reduced cell viability by more than 30%.

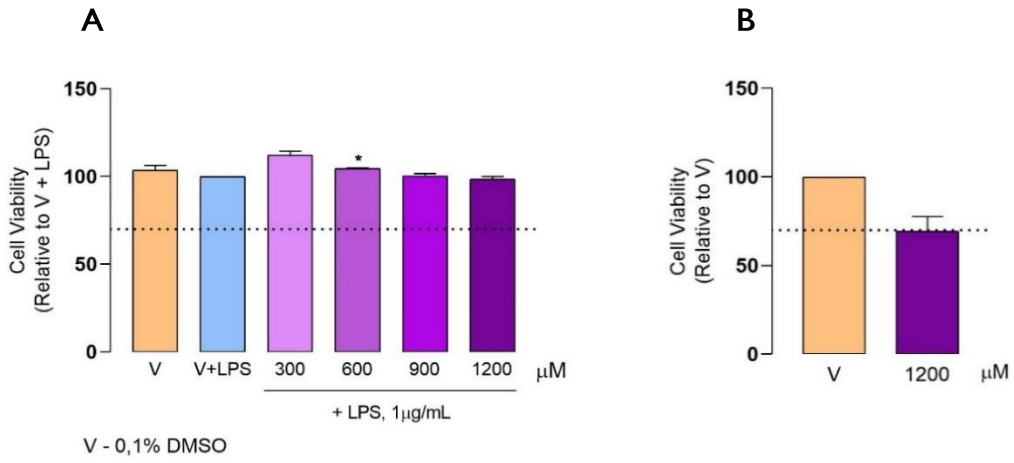

Figure 42. Effect of GM22 on cell viability. Raw 264.7 macrophage cultures were treated with vehicle (0.1% DMSO) or the concentrations of GM22 indicated, for 1 h before addition of 1 μg/mL LPS for 18 h. Control cells (V) were treated with the vehicle alone (0.1% DMSO) for the same period (**A**). Raw 264.7 macrophage cultures were treated with 1200 and 2400 μM of GM22 for 18 h in the absence of LPS; control cells (V) were treated with the vehicle alone (0,1% DMSO) for the same period (**B**). Each column represents the mean ± SEM. *p<0.05 relative to LPS-treated cells (V+LPS). The dotted line represents the 70% cell viability mark that is accepted, according to ISO 10993-5.

4.2.3.2 GM22 reduces LPS-induced NO production in Raw 264.7 macrophages

GM22 did not affect basal NO production when added to macrophage cultures in the absence of LPS (Fig. 43A), and it had a statistically significant effect on LPS-induced NO production. Results show that GM22 is able to reduce LPS-induced NO production in a concentration-dependent manner (Fig. 43B).

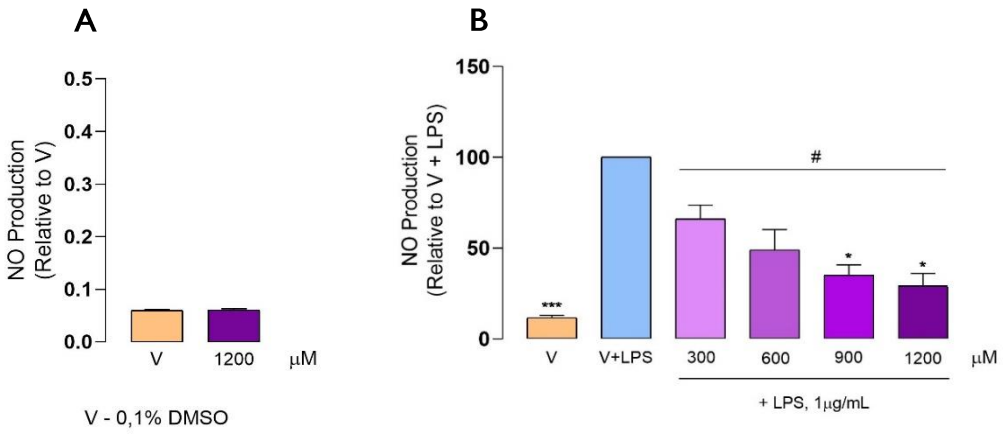

Figure 43. Effect of GM22 on NO production. Raw 264.7 macrophage cultures were treated with 1200 μM GM22 for 18 h in the absence of LPS; control cells (V) were treated with the vehicle alone (0,1% DMSO) for the same period (**A**). Raw 264.7 macrophage cultures were treated with the vehicle (0.1% DMSO) or the concentrations in the figure for 1 h before addition of 1 μg/mL LPS for 18 h. Control cells (V) were treated with the vehicle alone (0.1% DMSO) for the same period (**B**). Each column represents the mean ± SEM of three independent experiments. *p<0.05 and ***p<0.001 relative to LPS-treated cells (V+LPS). #p<0.05 relative to all the concentrations tested.

To evaluate the compound's potency, the concentration required to inhibit NO production by 50% (IC50) was determined as shown in Figure 44.

The IC_{50} value obtained for GM22 is 436.5 μM.

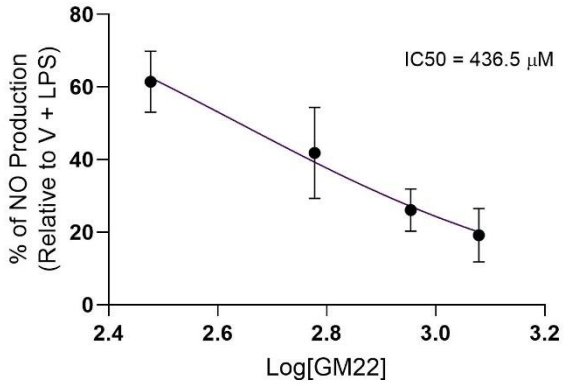

Figure 44. Concentration-response curve relative to inhibition of LPS-induced NO production by GM22 in the conditions depicted in Figure 43.

4.2.3.3 GM22 shows a tendency to inhibit LPS-induced iNOS expression on Raw 264.7 macrophages

Treatment with GM22 clearly decreased iNOS protein levels relative to cells treated with LPS alone, reaching statistical significance with the two highest concentrations (900 and 1200 µM). The concentrations of 300 and 600 µM probably did not reach statistical significance due to interassay variability and the small number of assays we could perform.

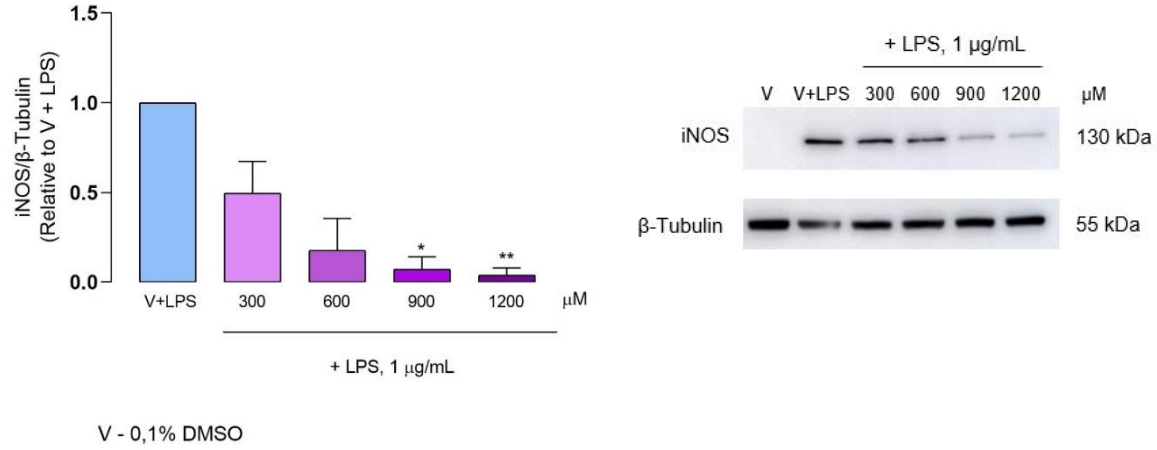

Figure 45. GM22 decreases LPS-induced iNOS protein levels in Raw 264.7 macrophages. Cells were treated with 1 µg/mL LPS for 18 h, following pre-treatment with the vehicle (0.1% DMSO) or GM22 concentrations indicated in the figure. Control cells (V) were treated with vehicle alone (0,1% DMSO) in the absence of LPS. Each column represents the mean ± SEM of three independent experiments. *p<0.05 and **p<0.01 relative to LPS-treated cells.

4.2.3.4 Effect of GM22 on LPS-induced pro-IL-1β protein levels in Raw 264.7 macrophages

As with GM2 and GM16f1, GM22 at concentrations of 600, 900 and 1200 µM shows a tendency to increase LPS-induced pro-IL-1β protein levels, but the differences did not reach statistical significance. This is probably due to the small number of assays that we could perform and the variability among them.

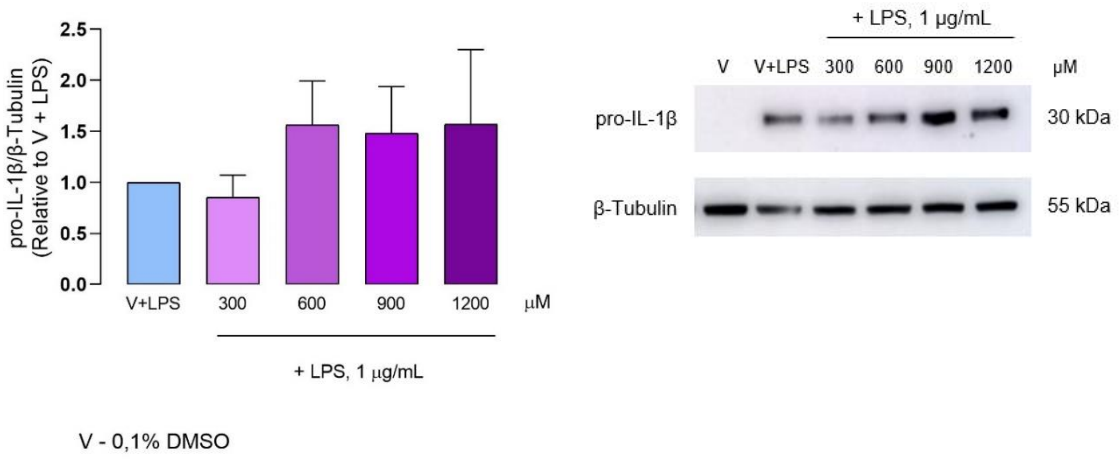

V - 0,1% DMSO

Figure 46. Effect of GM22 on LPS-induced pro-IL-1β protein levels in Raw 264.7 macrophages. Cells were treated with 1 μg/mL LPS for 18 h, following pre-treatment with the vehicle or the concentrations of GM22 indicated. Control cells (V) were treated with vehicle alone (0,1% DMSO) in the absence of LPS. Each column represents the mean ± SEM.

4.2.4 GM23

4.2.4.1 Cell viability of GM23-treated Raw 264.7 macrophages

Results in Fig. 47A show that in LPS-treated cells, none of the GM23 concentrations tested had cytotoxic effects. Although results for the concentration of 300 μM are statistically significant, the increase is very small and has no biological significance. Figure 47B represents cell viability results in cells treated with the test compound or the vehicle alone, in the absence of LPS. In these conditions, both GM23 concentrations tested in these conditions, 1200 and 2400 μM, reduced cell viability with statistical significance. However, only the concentration of 2400 μM can be considered cytotoxic, as it reduced cell viability by more than 30%. Since in the presence of LPS cell viability was not affected, this concentration was not excluded in subsequent experiments.

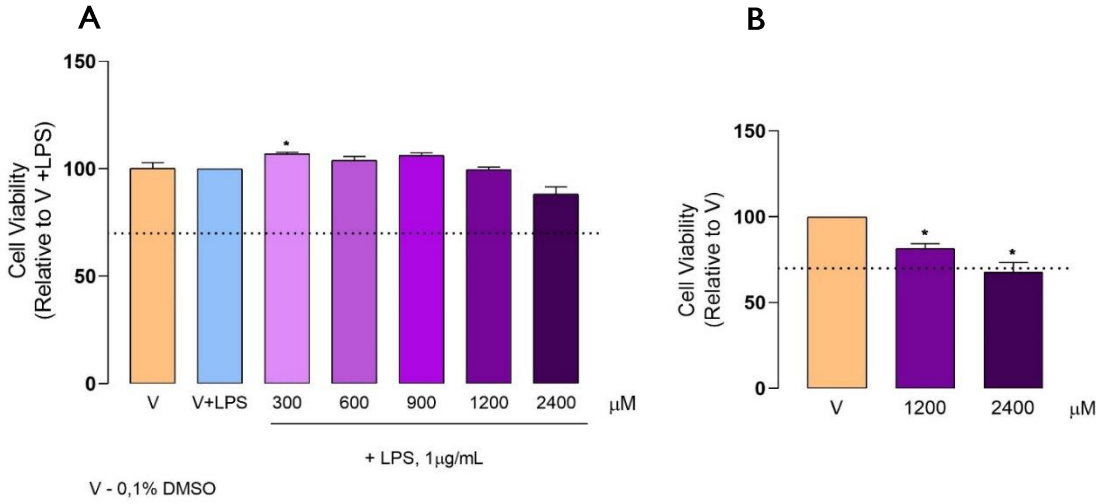

Figure 47. Effect of GM23 on cell viability. Raw 264.7 macrophage cultures were treated with the vehicle (0.1% DMSO) or the concentrations of GM23 indicated, for 1 h before addition of 1 μg/mL LPS for 18 h. Control cells (V) were treated with the vehicle alone (0.1% DMSO) for the same period (**A**). Raw 264.7 macrophage cultures were treated with 1200 and 2400 μM GM23 for 18 h in the absence of LPS; control cells (V) were treated with the vehicle alone (0,1% DMSO) for the same period (**B**). Each column represents the mean ± SEM of four independent experiments. *p<0.05 relative to LPS-treated cells (V+LPS). The dotted line represents the 70% cell viability mark that is accepted, according to ISO 10993-5.

4.2.4.2 GM23 reduces LPS-induced NO production in Raw 264.7 macrophages

GM23 did not affect basal NO production when added to macrophage cultures in the absence of LPS (Fig. 48A), and it had a statistically significant effect on LPS-induced NO production. Results show that all concentrations of GM23 tested were able to significantly reduce LPS-induced NO production (Fig. 48B).

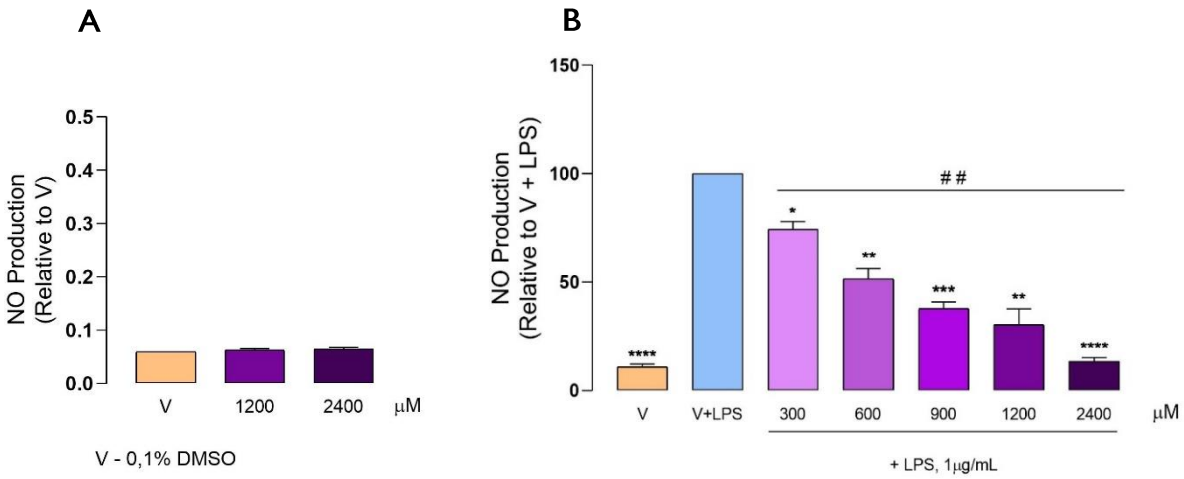

Figure 48. Effect of GM23 on NO production. Raw 264.7 macrophage cultures were treated with 1200 and 2400 µM GM23 for 18 h in the absence of LPS; control cells (V) were treated with the vehicle alone (0,1% DMSO) for the same period (**A**). Raw 264.7 macrophage cultures were treated with the vehicle or the concentrations of GM23 indicated for 1 h before addition of 1 µg/mL LPS for 18 h. Control cells (V) were treated with the vehicle alone (0.1% DMSO) for the same period (**B**). Each column represents the mean ± SEM of four independent experiments. *p<0.05, **p<0.001, ***p<0.001 and ****p<0.0001 relative to LPS-treated cells (V+LPS). ##p<0.01 relative to all the concentrations tested.

4.2.4.3 To evaluate GM23 potency, the concentration required to inhibit NO production by 50% (IC50) was determined as shown in Figure 49.

The IC_{50} value obtained for GM23 is 521.8 µM.

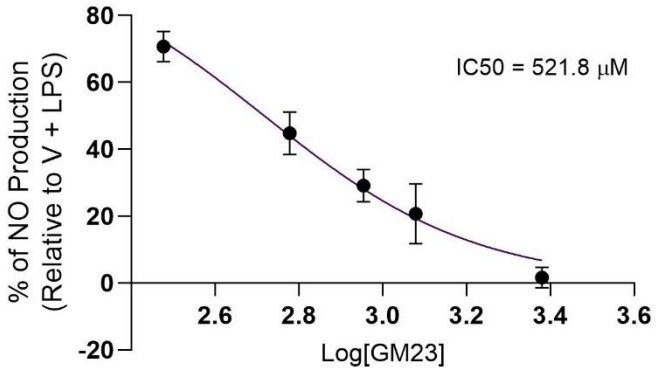

Figure 49. Concentration-response curve relative to inhibition of LPS-induced NO production by GM23 in the conditions depicted in Figure 48.

4.2.4.3 GM23 inhibits LPS-induced iNOS expression in Raw 264.7 macrophages

Treatment with concentrations of 600, 900, 1200 and 2400 µM decreased iNOS protein levels relative to cells treated with LPS alone with statistical significance (Fig. 50).

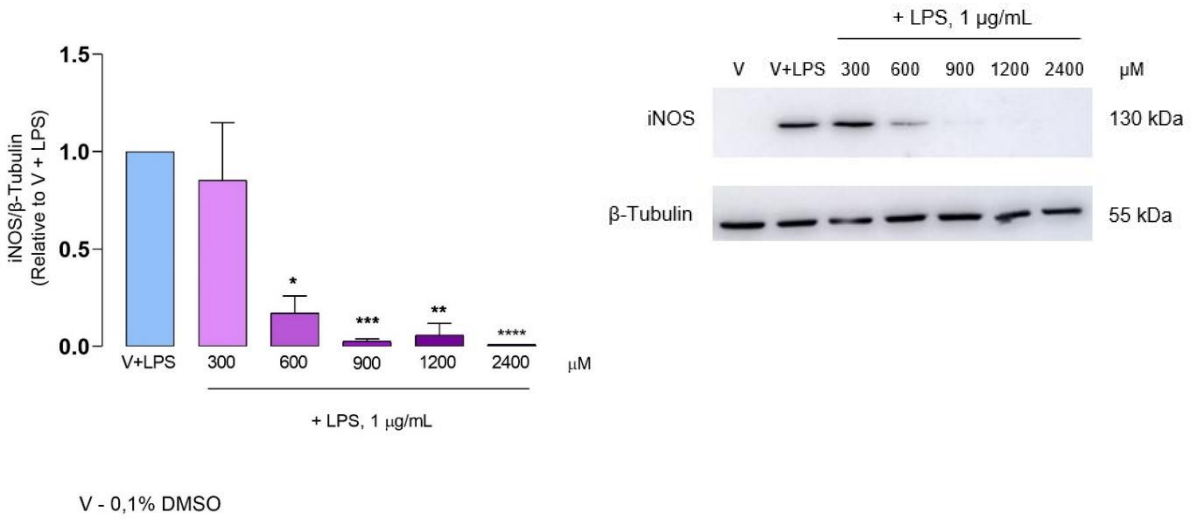

Figure 50. GM23 decreases LPS-induced iNOS protein levels in Raw 264.7 macrophages. Cells were treated with 1 µg/mL LPS for 18 h, following pre-treatment with GM23 concentrations indicated in the figure or the vehicle. Control cells (V) were treated with vehicle alone (0,1% DMSO) in the absence of LPS. Each column represents the mean ± SEM of three independent experiments. *p<0.05, **p<0.01, ***p<0.001 and ****p<0.0001 relative to LPS-treated cells.

4.2.4.4 GM23 decreases LPS-induced pro-IL-1β levels in Raw 264.7 macrophages

The results in Figure 21 show that concentrations of 600 and 1200 µM increased pro-IL-1β protein levels, but the differences did not reach statistical significance. However, the highest concentration of GM23, 2400 µM, was able to reduce pro-IL-1β levels with statistical significance.

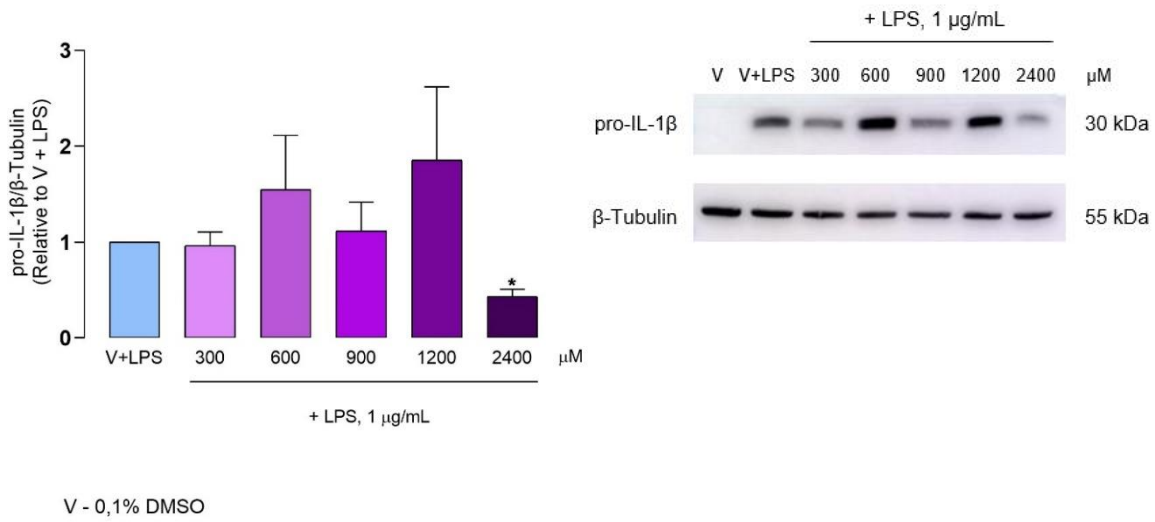

V - 0,1% DMSO

Figure 51. GM23 decreases LPS-induced pro-IL-1β protein levels in Raw 264.7 macrophages. Cells were treated with 1 μg/mL LPS for 18 h, following pre-treatment with the concentrations indicated or the vehicle. Control cells (V) were treated with vehicle alone (0,1% DMSO) in the absence of LPS. Each column represents the mean ± SEM of three independent experiments. *p<0.05 relative to LPS-treated cells.

5. Discussion and further perspectives

5.1 Semi-synthesis of ClAD7 derivatives

The main goal of this project was to design and synthetize new ClAD7 derivatives based on previous SAR studies, to obtain new compounds with improved pharmacokinetic and pharmacological properties. We were not able to biologically evaluate all the synthetized compounds, but the ones we did study – GM2, GM16f1, GM22 and GM23 – reached interesting results, as we will discuss below.

Some of the reactions resulted in products with an unsatisfactory yield, meaning that an optimization of the reaction processes may be needed to achieve better outcomes. However, we unfortunately did not have the time to optimize the experimental procedures.

As previously explained, since most common protocols for the synthesis of β-alkoxy alcohols is the ring opening of epoxides with a suitable alcohol under strongly acidic or basic conditions it is possible to perform the reaction under mild catalytic conditions (Leitão *et al.*, 2008). Therefore, we performed the nucleophilic ring-opening of the epoxide of GM3 or GM4 using MeOH and EtOH, obtaining 8 different products and their respective diastereoisomers. After analyzing all the compounds' ^{1}H NMR and ^{13}C NMR spectra and the obtained yields for each reaction, we were able to conclude that the ring-opening of the epoxide with MeOH had a better outcome than with EtOH. The ring-opening of the epoxide in the presence of EtOH generated products with considerable amounts of impurities that were not eliminated after flash chromatography.

One of the disadvantages of nucleophilic ring-opening of racemic epoxides with alcohols is that this procedure generates four products – two pairs of diastereoisomers – as the epoxide is obtained by a non-stereoselective method. We were able to separate the two different pairs of compounds (regioisomers), but we could not separate the diastereoisomers from each other. In order to obtain these compounds separately, instead of converting the alkene bond to an (racemic) epoxide using m-CPBA, we should use a stereoselective method of epoxidation. The Sharpless asymmetric epoxidation has been highlighted in the scientific community since it not only forms chiral epoxides in high yields and enantioselectivity, but also produces diastereo- and regioselective epoxidation of alkenes in the presence of multiple sterically-similar alkenes, which is classified as substrate-directed reaction (Sawano and Yamamoto, 2020). The Sharpless method stereoselectively converts a prochiral allylic alcohol to an epoxide using titanium isopropoxide [$Ti(OiPr)_4$], t-butyl hydroperoxide (TBHP), and an appropriate chiral diethyl tartrate (DET). This protocol includes some advantages over

stoichiometric reactions, in particular the easier isolation of the products and enhanced yields (Heravi, Lashaki and Poorahmad, 2015).

In general, we were able to modify CIAD7's structure based on previous SAR studies, in order to create new compounds that were submitted to a biological evaluation to further understand if their pharmacological characteristics were improved relatively to CIAD7.

5.2 Pharmacological characterization of the anti-inflammatory properties of CIAD7 derivatives

As previously stated in this project, a low-grade chronic inflammation state is common to a wide range of aging-related diseases and the currently available therapies only allow the management of inflammation-related symptoms for relatively short periods. Therefore, several efforts are being made to find and study new compounds with potential anti-inflammatory properties without the side effects related to the currently available drugs.

The main goal of this work was to study the anti-inflammatory properties of the synthetized compounds, by evaluating their capacity to inhibit NO production and decrease the protein levels of iNOS and pro-IL-1β.

First, viability assays were performed in Raw 264.7 cells to understand if the chosen concentrations of the tested compounds were safe and did not present cytotoxic effects. In fact, none of the concentrations tested for all the evaluated compounds had cytotoxic effects in the presence of LPS. However, in the absence of LPS, GM16f1, GM22 and GM23 showed a reduction in cell viability. However, these results may not necessarily indicate that these compounds are toxic in the absence of LPS as it has a significant effect on cell proliferation (Shi *et al.*, 2016). To further understand if the observed effects represent a reduction in cell proliferation and not cell toxicity, there are several experiments that could be performed. 5-bromo-2'-deoxyuridine (BrDU) or 5-ethynyl-2'-deoxyuridine (EdU) cytometry assays are two great examples of well-established cell proliferation studying methods. BrdU is a thymidine analog that can incorporate into newly replicated DNA of S-phase cells and it has a high labeling efficiency. Usually, BrdU incorporation into DNA is detected by anti-BrdU antibodies (Diermeier-Daucher *et al.*, 2009; Yin *et al.*, 2014). On the other hand, EdU is another thymidine analogue that is incorporated into actively dividing cells, but is not detected by antibodies. This assay is based on a copper-catalyzed reaction that adds a fluorescent azide to an alkyne group on the DNA incorporated EdU ("click" reaction) (Alvarez *et al.*, 2020; O'Hara *et al.*, 2019). With any of these methods, it would be possible to confirm if GM16f1, GM22 and GM23 have cytotoxic effects in the absence of LPS or if there is a decrease in cell proliferation, resulting

in a decrease in metabolic activity by the resazurin assay. Another way to prove this is by quantifying dead cells by the Annexin V affinity assay or the Calcein-AM assay. Annexin V is a member of a family of calcium-dependent phospholipid binding proteins that binds to phosphatidylserine (PS), which is an integral component of the plasma membrane that is confined to the inner leaflet of the membrane in healthy cells. PS translocates to the outer leaflet of the plasma membrane during apoptosis. Staining cells simultaneously with annexin V labeled with the fluorochrome fluorescein isothiocyanate (FITC) and the non-vital dye propidium iodide (PI) allows the discrimination among healthy cells, early apoptotic cells and late apoptotic or necrotic cells (Kupcho *et al.*, 2019; Marder *et al.*, 2014). On the other hand, Calcein-AM is a non-fluorescent lipophilic ester that easily penetrates cellular membranes and is rapidly cleaved by unspecific cytosolic esterases. Live cells are distinguished by the presence of ubiquitous intracellular esterase activity, determined by enzyme conversion of the non-fluorescent cell permeant calcein-AM to the intensely green fluorescent calcein. To distinguish live (brightly stained by calcein) from dead cells, a membrane impermeable DNA dye, such as Ethidium homodimer or Propidium Iodide, which stain nucleic acids. by intercalating between the base pairs, is used as it only enters cells with membrane damages, producing a bright red fluorescence in dead cells (Decherchi, Cochard and Gauthier, 1997; Tenopoulou *et al.*, 2007). The obtained results confirmed that all the tested compounds are able to reduce LPS-induced iNOS protein levels and NO production in a concentration-dependent manner. Nonetheless, these compounds show significant differences in potency relative to their ability to inhibit NO production. GM23 was found to be the most potent (IC_{50}= 436.5 μM), followed by its enantiomer, GM22 (IC_{50}= 521.8 μM) and with much lower potencies, by GM16f1 (IC_{50}= 1010 μM) and GM2 (IC_{50}= 1046 μM). Further studies, namely real time RT-PCR, would be important to elucidate whether the decrease in iNOS protein levels is due to inhibition of transcription or of the enzyme activity.

On the other hand, the effect of the test compounds in pro-IL-1β protein levels is ambiguous and no solid conclusions can be made. Indeed, in general, none of the test compounds had a statistically significant effect in the levels of this protein, but most of them, in at least one of the concentrations tested, caused an increase of those levels, while at the highest concentration tested, GM16f1 and GM23 showed a significant reduction. Increasing the number of experiments would help in determining whether or not the increase is relevant, but other mechanisms may be involved. As mentioned in the Introduction, pro-IL-1β is cleaved by the pro-inflammatory protease, caspase-1. The activation of caspase-1 occurs via recruitment to the inflammasome, and after the processing of pro-IL-1β by caspase-1, mature IL-1β is secreted from the cell (Lopez-Castejon and Brough, 2011). At any given time, pro-IL-

1β levels in the cell depend on the synthesis and secretion of mature IL-1β after its partial hydrolysis in the inflammasome. The increase in pro-IL-1 β levels can be due to inhibition of the inflammasome and consequent intracellular accumulation. Another explanation could be increased *IL-1β* gene expression induced by the test compounds, but this is improbable because the highest concentration of two test compounds significantly decreased those levels, suggesting the opposite effect, that is, inhibition of *IL-1β* gene expression. To elucidate these questions, the effects of the test compounds in the activity and protein levels of caspase-1 could be assessed, along with IL-1β mRNA levels which would show if and how the test compounds affect gene transcription. To further confirm potential inhibition of the inflammasome, the levels of secreted mature IL-1β could also be measured in culture supernatants.

The small amounts of compounds that we obtained only allowed us to generally perform 3 assays per each experiment. The small number of assays that we could perform was one of the main limitations of this project. Furthermore, the variability among experiments, particularly in the IL-1β protein levels assessed by Western Blot, lead us to inconclusive results. Increasing the number of assays per experiment would give more robust results and would allow us to understand better how the compounds modulate IL-1β production.

6. Conclusion

Through the course of this project, we were able to synthetize several ClAD7 derivatives and evaluate the anti-inflammatory properties of GM2, GM16f1, GM22 and GM23 in an *in vitro* model of inflammation. The obtained results lead us to conclude that these compounds, besides not having significant cytotoxic effects in concentrations up to 2400 μM, have indeed some anti-inflammatory properties, as they clearly reduced the levels of a major pro-inflammatory protein, iNOS, induced by LPS. Furthermore, although unclear, the results obtained for another important inflammatory mediator, IL-1β, suggest that these compounds may inhibit its gene expression, as well as its processing and secretion by inhibiting the inflammasome or, directly, caspase-1.

This study paves the way for further *in vitro* studies aimed at fully understanding the anti-inflammatory effects of these compounds and the underlying mechanisms and determining whether the chemical modifications of ClAD7 introduced have any advantages over the parent compound.

7. References

ADCOCK, Ian M.; MUMBY, Sharon - Glucocorticoids. Em **Handbook of Experimental Pharmacology** Available in http://link.springer.com/10.1007/164_2016_98. ISBN 978-3-319-29806-1. p. 171–196.

ADLI, Mazhar *et al.* - IKKα and IKKβ each function to regulate NF-κB activation in the TNF-induced/canonical pathway. **PLoS ONE**. ISSN 19326203. 5:2 (2010) 1–7. doi: 10.1371/journal.pone.0009428.

ALVAREZ, Karla Luciá F. *et al.* - An EdU-based flow cytometry assay to evaluate chicken T lymphocyte proliferation. **BMC Veterinary Research**. . ISSN 17466148. 16:1 (2020) 1–12. doi: 10.1186/s12917-020-02433-0.

ANDERS, Hans Joachim - Of Inflammasomes and alarmins: IL-1β and IL-1α in kidney disease. **Journal of the American Society of Nephrology**. . ISSN 15333450. 27:9 (2016) 2564–2575. doi: 10.1681/ASN.2016020177.

AZAB, Abdullatif; NASSAR, Ahmad; AZAB, Abed N. - Anti-inflammatory activity of natural products. **Molecules**. ISSN 14203049. 21:10 (2016) 1–19. doi: 10.3390/molecules21101321.

BARBÉ-TUANA, Florencia *et al.* - The interplay between immunosenescence and age-related diseases. **Seminars in Immunopathology**. ISSN 18632300. 42:5 (2020) 545–557. doi: 10.1007/s00281-020-00806-z.

BARNES, Peter J. - Corticosteroids: The drugs to beat. **European Journal of Pharmacology**. ISSN 00142999. 533:1–3 (2006) 2–14. doi: 10.1016/j.ejphar.2005.12.052.

BEKTAS, Arsun *et al.* - Aging, inflammation and the environment. **Experimental Gerontology**. ISSN 18736815. 105:October (2018) 10–18. doi: 10.1016/j.exger.2017.12.015.

BEUTLER, John A. - Natural products as a foundation for drug discovery. **Current Protocols in Pharmacology**. ISSN 19348282. SUPPL. 46 (2009) 1–21. doi: 10.1002/0471141755.ph0911s46.

BINDU, Samik; MAZUMDER, Somnath; BANDYOPADHYAY, Uday - Non-steroidal anti-inflammatory drugs (NSAIDs) and organ damage: A current perspective. **Biochemical Pharmacology**. ISSN 18732968. 180:April (2020). doi: 10.1016/j.bcp.2020.114147.

BOURS, Vincent *et al.* - The NF-κB transcription factor and cancer: high expression of NF-κB- and IκB-related proteins in tumor cell lines. **Biochemical Pharmacology**. . ISSN 00062952.

47:1 (1994) 145–149. doi: 10.1016/0006-2952(94)90448-0.

BRYAN, Nathan S.; GRISHAM, Matthew B. - Methods to detect nitric oxide and its metabolites in biological samples. **Free Radical Biology and Medicine**. . ISSN 08915849. 43:5 (2007) 645–657. doi: 10.1016/j.freeradbiomed.2007.04.026.

BUDUNOVA, Irina V *et al.* - Increased expression of p50-NF-κB and constitutive activation of NF-κB transcription factors during mouse skin carcinogenesis. **Oncogene**. ISSN 09509232. 18:52 (1999) 7423–7431. doi: 10.1038/sj.onc.1203104.

CANDORE, G. *et al.* - Low Grade Inflammation as a Common Pathogenetic Denominator in Age-Related Diseases: Novel Drug Targets for Anti-Ageing Strategies and Successful Ageing Achievement. **Current Pharmaceutical Design**. . ISSN 13816128. 16:6 (2010) 584–596. doi: 10.2174/138161210790883868.

CAREY, Francis A.; SUNDBERG, Richard J. - **Advanced Organic Chemistry**. 5th Editio ed. Charlottesville, VA : Springer International Publishing, 2007. ISBN 978-0-387-44899-3.

CAVAILLON, J. M. - Cytokines and macrophages. **Biomedicine & Pharmacotherapy**. . ISSN 07533322. 48:10 (1994) 445–453. doi: 10.1016/0753-3322(94)90005-1.

CHAMBERLAIN, Paul H. - Identification of an Alcohol with 13C NMR Spectroscopy. **Journal of Chemical Education**. 90 (2013) 1365–1367.

CHEN, Jichao *et al.* - Insights into drug discovery from natural products through structural modification. **Fitoterapia**. ISSN 18736971. 103:2015) 231–241. doi: 10.1016/j.fitote.2015.04.012.

CHEN, Linlin *et al.* - Inflammatory responses and inflammation-associated diseases in organs. **Oncotarget**. ISSN 19492553. 9:6 (2018) 7204–7218. doi: 10.18632/oncotarget.23208.

CINELLI, Maris A. *et al.* - Inducible nitric oxide synthase: Regulation, structure, and inhibition. **Medicinal Research Reviews**. ISSN 10981128. 40:1 (2020) 158–189. doi: 10.1002/med.21599.

COOPER, Cyrus *et al.* - Safety of Oral Non-Selective Non-Steroidal Anti-Inflammatory Drugs in Osteoarthritis: What Does the Literature Say? **Drugs and Aging**. ISSN 11791969. 36:s1 (2019) 15–24. doi: 10.1007/s40266-019-00660-1.

CRAGG, Gordon M.; NEWMAN, David J. - Natural products: A continuing source of novel drug leads. **Biochimica et Biophysica Acta - General Subjects**. ISSN 03044165. 1830:6

(2013) 3670–3695. doi: 10.1016/j.bbagen.2013.02.008.

DECHERCHI, Patrick; COCHARD, Philippe; GAUTHIER, Patrick - Dual staining assessment of Schwann cell viability within whole peripheral nerves using calcein-AM and ethidium homodimer. **Journal of Neuroscience Methods**. ISSN 01650270. 71:2 (1997) 205–213. doi: 10.1016/S0165-0270(96)00146-X.

DIERMEIER-DAUCHER, Simone *et al.* - Cell type specific applicability of 5-ethynyl-2′-deoxyuridine (EDU) for dynamic proliferation assessment in flow cytometry. **Cytometry Part A**. . ISSN 15524922. 75:6 (2009) 535–546. doi: 10.1002/cyto.a.20712.

DINARELLO, Charles A.; SIMON, Anna; MEER, Jos W. M. VAN DER - Treating inflammation by blocking interleukin-1 in a broad spectrum of diseases. **Nature Reviews Drug Discovery**. ISSN 1474-1776. 11:8 (2012) 633–652. doi: 10.1038/nrd3800.

ECKRICH, Ralf *et al.* - Stereoselective epoxidation of cyclohexa-anellated triquinacenes with iodine/silver(I) oxide as compared to m-chloroperbenzoic acid. **Journal of Organic Chemistry**. ISSN 00223263. 61:11 (1996) 3839–3843. doi: 10.1021/jo952265f.

FEI, Junliang *et al.* - Luteolin inhibits IL-1β-induced inflammation in rat chondrocytes and attenuates osteoarthritis progression in a rat model. **Biomedicine and Pharmacotherapy**. ISSN 19506007. 109:May 2018 (2019) 1586–1592. doi: 10.1016/j.biopha.2018.09.161.

FIGUEIREDO, Sandra A. C. *et al.* - Novel celastrol derivatives with improved selectivity and enhanced antitumour activity: Design, synthesis and biological evaluation. **European Journal of Medicinal Chemistry**. ISSN 17683254. 138:2017) 422–437. doi: 10.1016/j.ejmech.2017.06.029.

FORMAN, K. *et al.* - Influence of aging and growth hormone on different members of the NFkB family and IkB expression in the heart from a murine model of senescence-accelerated aging. **EXG**. ISSN 0531-5565. 73:2016) 114–120. doi: 10.1016/j.exger.2015.11.005.

FUENTES, Eduardo *et al.* - Immune system dysfunction in the elderly. **Anais da Academia Brasileira de Ciencias**. ISSN 16782690. 89:1 (2017) 285–299. doi: 10.1590/0001-3765201720160487.

GARCIA, Antequera - **Enantioselective epoxidation of simple alkenes based upon the concept of pi-interactions-facial recognition**. Université Catholique de Louvain, 2005 Available in http://hdl.handle.net/2078.1/5308.

GARLANDA, Cecilia; DINARELLO, Charles A.; MANTOVANI, Alberto - The Interleukin-1

Family: Back to the Future. **Immunity**. ISSN 10747613. 39:6 (2013) 1003–1018. doi: 10.1016/j.immuni.2013.11.010.

GEISSMANN, F. *et al.* - Development of Monocytes, Macrophages, and Dendritic Cells. **Science**. ISSN 0036-8075. 327:5966 (2010) 656–661. doi: 10.1126/science.1178331.

GERMIC, Nina *et al.* - Regulation of the innate immune system by autophagy: neutrophils, eosinophils, mast cells, NK cells. **Cell Death and Differentiation**. ISSN 14765403. 26:4 (2019) 703–714. doi: 10.1038/s41418-019-0295-8.

GERMIC, Nina *et al.* - Regulation of the innate immune system by autophagy: monocytes, macrophages, dendritic cells and antigen presentation. **Cell Death and Differentiation**. ISSN 14765403. 26:4 (2019) 715–727. doi: 10.1038/s41418-019-0297-6.

GILMORE, T. D. - Introduction to NF-kB: players, pathways, perspectives. **Oncogene** (2006) 6680–6684. doi: 10.1038/sj.onc.1209954.

GUO, Zongru - The modification of natural products for medical use. **Acta Pharmaceutica Sinica B**. ISSN 22113843. 7:2 (2017) 119–136. doi: 10.1016/j.apsb.2016.06.003.

GUZIK, T. J.; KORBUT, R. - Nitric oxide and superoxide in inflammation and immune regulation. **Journal of Physiology and Pharmacology**. 54:4 (2003) 469–487.

HARVEY, Alan L. - Natural products in drug discovery. **Drug Discovery Today**. ISSN 13596446. 13:19–20 (2008) 894–901. doi: 10.1016/j.drudis.2008.07.004.

HELENIUS, Merja *et al.* - Characterization of aging-associated up-regulation of constitutive nuclear factor-κB binding activity. **Antioxidants and Redox Signaling**. ISSN 15230864. 3:1 (2001) 147–156. doi: 10.1089/152308601750100669.

HENRICH, Curtis J.; BEUTLER, John A. - Matching the power of high throughput screening to the chemical diversity of natural products. **Natural Product Reports**. ISSN 0265-0568. 30:10 (2013) 1284. doi: 10.1039/c3np70052f.

HERAVI, Majid M.; LASHAKI, Tahmineh Baie; POORAHMAD, Nasim - Applications of Sharpless asymmetric epoxidation in total synthesis. **Tetrahedron Asymmetry**. ISSN 1362511X. 26:8–9 (2015) 405–495. doi: 10.1016/j.tetasy.2015.03.006.

KANG, Ki Sung - Phytochemical constituents of medicinal plants for the treatment of chronic inflammation. **Biomolecules**. ISSN 2218273X. 11:5 (2021) 11–12. doi: 10.3390/biom11050672.

KENNEDY, Brian K. *et al.* - Geroscience: Linking aging to chronic disease. **Cell**. ISSN 10974172. 159:4 (2014) 709–713. doi: 10.1016/j.cell.2014.10.039.

KIELBIK, Michal; SZULC-KIELBIK, Izabela; KLINK, Magdalena - The potential role of iNOS in ovarian cancer progression and chemoresistancefile. **International Journal of Molecular Sciences**. ISSN 14220067. 20:7 (2019). doi: 10.3390/ijms20071751.

KINGHORN, A. Douglas - The role of pharmacognosy in modern medicine. **Expert Opinion on Pharmacotherapy**. ISSN 14656566. 3:2 (2002) 77–79. doi: 10.1517/14656566.3.2.77.

KLEINERT, Hartmut; ART, Julia; PAUTZ, Andrea - Regulation of the Expression of Inducible Nitric Oxide Synthase. **Nitric Oxide**. 384:November (2010) 211–267. doi: 10.1016/B978-0-12-373866-0.00007-1.

KRÓL, Magdalena; KEPINSKA, Marta - Human nitric oxide synthase—its functions, polymorphisms, and inhibitors in the context of inflammation, diabetes and cardiovascular diseases. **International Journal of Molecular Sciences**. ISSN 14220067. 22:1 (2021) 1–18. doi: 10.3390/ijms22010056.

KUPCHO, Kevin *et al.* - A real-time, bioluminescent annexin V assay for the assessment of apoptosis. **Apoptosis**. ISSN 1573675X. 24:1–2 (2019) 184–197. doi: 10.1007/s10495-018-1502-7.

LEITÃO, Alcino J. L. *et al.* - Hydrazine sulphate: a cheap and efficient catalyst for the regioselective ring-opening of epoxides. A metal-free procedure for the preparation of β-alkoxy alcohols. **Tetrahedron Letters**. ISSN 00404039. 49:10 (2008) 1694–1697. doi: 10.1016/j.tetlet.2007.12.121.

LI, Qingxin; KANG, Cong Bao - A practical perspective on the roles of solution NMR spectroscopy in drug discovery. **Molecules**. ISSN 14203049. 25:13 (2020) 1–19. doi: 10.3390/molecules25132974.

LI, Yanqun *et al.* - The effect of developmental and environmental factors on secondary metabolites in medicinal plants. **Plant Physiology and Biochemistry**. ISSN 09819428. 148:June 2019 (2020) 80–89. doi: 10.1016/j.plaphy.2020.01.006.

LINTHOUT, Sophie VAN; MITEVA, Kapka; TSCHÖPE, Carsten - Crosstalk between fibroblasts and inflammatory cells. **Cardiovascular Research**. ISSN 17553245. 102:2 (2014) 258–269. doi: 10.1093/cvr/cvu062.

LIU, Dora *et al.* - A practical guide to the monitoring and management of the complications of

systemic corticosteroid therapy. **Allergy, Asthma and Clinical Immunology**. ISSN 17101492. 9:1 (2013) 1. doi: 10.1186/1710-1492-9-30.

LIU, Xin - **10.3 Reactions of Alkenes: Addition of Water (or Alcohol) to Alkenes.** Organic Chemistry I. Available in https://kpu.pressbooks.pub/organicchemistry/chapter/10-3-reactions-of-alkenes-part-ii-multiple-step-process/.

LOPEZ-CASTEJON, Gloria; BROUGH, David - Understanding the mechanism of IL-1β secretion. **Cytokine and Growth Factor Reviews**. ISSN 13596101. 22:4 (2011) 189–195. doi: 10.1016/j.cytogfr.2011.10.001.

MANDAI, Hiroki *et al.* - Enantioselective acyl transfer catalysis by a combination of common catalytic motifs and electrostatic interactions. **Nature Communications**. 7:2016) 1–11. doi: 10.1038/ncomms11297.

MARDER, Laura S. *et al.* - Production of recombinant human annexin V by fed-batch cultivation. **BMC Biotechnology**. ISSN 14726750. 14:2014). doi: 10.1186/1472-6750-14-33.

MATHUR, Sunil; HOSKINS, Clare - Drug development: Lessons from nature. **Biomedical Reports**. ISSN 2049-9434. 6:6 (2017) 612–614. doi: 10.3892/br.2017.909.

MCKINNEY, James D. *et al.* - The practice of structure activity relationships (SAR) in toxicology. **Toxicological Sciences**. . ISSN 10966080. 56:1 (2000) 8–17. doi: 10.1093/toxsci/56.1.8.

MENDES, Alexandrina Ferreira; CRUZ, Maria Teresa; GUALILLO, Oreste - Editorial: The Physiology of Inflammation—The Final Common Pathway to Disease. **Frontiers in Physiology**. ISSN 1664-042X. 9:December (2018). doi: 10.3389/fphys.2018.01741.

MORIMOTO, Junki *et al.* - Improvement in aqueous solubility of achiral symmetric cyclofenil by modification to a chiral asymmetric analog. **Scientific Reports**. . ISSN 20452322. 11:1 (2021) 1–8. doi: 10.1038/s41598-021-92028-y.

O'HARA, Rosalie E. *et al.* - Three Optimized Methods for In Situ Quantification of Progenitor Cell Proliferation in Embryonic Kidneys Using BrdU, EdU, and PCNA. **Canadian Journal of Kidney Health and Disease**. ISSN 20543581. 6:2019). doi: 10.1177/2054358119871936.

OH, Jung Hwa *et al.* - Withaferin A inhibits iNOS expression and nitric oxide production by Akt inactivation and down-regulating LPS-induced activity of NF-κB in RAW 264.7 cells. **European Journal of Pharmacology**. ISSN 00142999. 599:1–3 (2008) 11–17. doi: 10.1016/j.ejphar.2008.09.017.

OHADOMA, Sylvester Chika; AKAH, Peter; MICHAEL, Henry Ukachukwu - Limitations of non-steroidal anti-inflammatory drugs and the utility of natural products for antinociceptive and antiexudative effects. **European Journal of Pharmaceutical and Medical Research**. July (2020).

OKEKE, Emeka B.; UZONNA, Jude E. - The pivotal role of regulatory T cells in the regulation of innate immune cells. **Frontiers in Immunology**. ISSN 16643224. 10:APR (2019) 1–12. doi: 10.3389/fimmu.2019.00680.

PAGARE, Saurabh *et al.* - Secondary metabolites of plants and their role: Overview. **Current Trends in Biotechnology and Pharmacy**. ISSN 22307303. 9:3 (2015) 293–304.

PASPARAKIS, Manolis - Regulation of tissue homeostasis by NF - κ B signalling : implications for inflammatory diseases. **Nature Reviews Immunology**. ISSN 1474-1733. 9:11 (2009) 778–788. doi: 10.1038/nri2655.

PRÄBST, Konstantin *et al.* - Basic colorimetric proliferation assays: MTT, WST, and resazurin. **Methods in Molecular Biology**. ISSN 10643745. 1601:2017) 1–17. doi: 10.1007/978-1-4939-6960-9_1.

PRASAD, Sahdeo; SUNG, Bokyung; AGGARWAL, Bharat B. - Age-associated chronic diseases require age-old medicine: Role of chronic inflammation. **Preventive Medicine**. ISSN 00917435. 54:SUPPL. (2012) S29–S37. doi: 10.1016/j.ypmed.2011.11.011.

SALMERÓN-MANZANO, Esther; GARRIDO-CARDENAS, Jose Antonio; MANZANO-AGUGLIARO, Francisco - Worldwide research trends on medicinal plants. **International Journal of Environmental Research and Public Health**. ISSN 16604601. 17:10 (2020). doi: 10.3390/ijerph17103376.

SAWANO, Takahiro; YAMAMOTO, Hisashi - Regio- and Enantioselective Substrate-Directed Epoxidation. **European Journal of Organic Chemistry**. ISSN 10990690. 2020:16 (2020) 2369–2378. doi: 10.1002/ejoc.201901656.

SCHÄCKE, Heike; DÖCKE, Wolf Dietrich; ASADULLAH, Khusru - Mechanisms involved in the side effects of glucocorticoids. **Pharmacology and Therapeutics**. ISSN 01637258. 96:1 (2002) 23–43. doi: 10.1016/S0163-7258(02)00297-8.

SHI, Huiyu *et al.* - The in vitro effect of lipopolysaccharide on proliferation, inflammatory factors and antioxidant enzyme activity in bovine mammary epithelial cells. **Animal Nutrition**. ISSN 24056383. 2:2 (2016) 99–104. doi: 10.1016/j.aninu.2016.03.005.

TABAS, I.; GLASS, C. K. - Anti-Inflammatory Therapy in Chronic Disease: Challenges and Opportunities. **Science**. ISSN 0036-8075. 339:6116 (2013) 166–172. doi: 10.1126/science. 1230720.

TENOPOULOU, Margarita *et al.* - Does the calcein-AM method assay the total cellular «labile iron pool» or only a fraction of it? **Biochemical Journal**. ISSN 02646021. 403:2 (2007) 261–266. doi: 10.1042/BJ20061840.

WILSON, Rebecca M.; DANISHEFSKY, Samuel J. - Small molecule natural products in the discovery of therapeutic agents: The synthesis connection. **Journal of Organic Chemistry**. ISSN 00223263. 71:22 (2006) 8329–8351. doi: 10.1021/jo0610053.

WINK, Michael - Modes of Action of Herbal Medicines and Plant Secondary Metabolites. **Medicines**. ISSN 2305-6320. 2:3 (2015) 251–286. doi: 10.3390/medicines2030251.

XIAO, Zhiyan; MORRIS-NATSCHKE, Susan L.; LEE, Kuo-Hsiung - Strategies for the Optimization of Natural Leads to Anticancer Drugs or Drug Candidates. **Medicinal Research Reviews**. ISSN 01986325. 36:1 (2016) 32–91. doi: 10.1002/med.21377.

YAO, Hong *et al.* - The structural modification of natural products for novel drug discovery. **Expert Opinion on Drug Discovery**. ISSN 1746045X. 12:2 (2017) 121–140. doi: 10.1080/17460441.2016.1272757.

YIN, Lei Miao *et al.* - Simultaneous application of BrdU and WST-1 measurements for detection of the proliferation and viability of airway smooth muscle cells. **Biological Research**. ISSN 07176287. 47:1 (2014) 1–5. doi: 10.1186/0717-6287-47-75.